

EVOLUTION OF THE INTERNAL DYNAMICS OF GALAXY CLUSTERS

MARISA GIRARDI AND MARINO MEZZETTI

Dipartimento di Astronomia, Università degli Studi di Trieste, Via Tiepolo 11, I-34131 Trieste, Italy
E-mail: girardi@ts.astro.it, mezzetti@ts.astro.it

ABSTRACT

We consider a sample of 51 distant galaxy clusters at $0.15 \lesssim z \lesssim 0.9$ ($\langle z \rangle \sim 0.3$), each cluster having at least 10 galaxies with available redshift in the literature. We select member galaxies, analyze the velocity dispersion profiles, and evaluate in a homogeneous way cluster velocity dispersions and virial masses.

We apply the same procedures already recently applied on a sample of nearby clusters ($z < 0.15$, Girardi et al. 1998b) in order to properly analyze the possible dynamical evolution of galaxy clusters. We remark problems induced by the poor sampling and the small spatial extension of the sampled cluster region in the computation of velocity dispersion.

We do not find any significant difference between nearby and distant clusters. In particular, we consider the galaxy spatial distribution, the shape of the velocity dispersion profile, and the relations between velocity dispersion and X-ray luminosity and temperature. Our results imply little dynamical evolution in the range of redshift spanned by our cluster sample, and suggest that the typical redshift of cluster formation is higher than that of the sample we analyze.

Subject headings: galaxies: distances and redshifts - X-rays: galaxies - cosmology: observations.

1 INTRODUCTION

The knowledge of the properties of galaxy clusters and of their possible evolution plays an important role in the study of large scale structure formation constraining cosmological models (e.g., Henry et al. 1992; Oukbir & Blanchard 1992; Colafrancesco & Vittorio 1994; Eke, Cole, & Frenk 1996). The evolution of their statistical properties have been studied previously. In particular, there is no evidence of evolution in the bulk of population of X-ray selected clusters (out to $z \sim 0.8$; e.g., Burke et al. 1997; Jones et al. 1998; Rosati et al. 1998), with evidence for a negative evolution of the X-ray luminosity function holding only for the brightest objects (e.g., Gioia et al. 1990; Vikhlinin et al. 1998; Rosati et al. 2000). There is evidence of a mild evolution of the cluster X-ray temperature function (out to $z \sim 0.8$, Henry 1997; Donahue & Voit 1999), and of somewhat larger evolution of the internal velocity–dispersion function (Carlberg et al. 1997b; Borgani et al. 1999). Other recent studies concern the relations between X-ray properties or between X-ray and optical properties finding no evidence of evolutions (out to $z \sim 0.4 - 0.5$; e.g., Mushotzky & Scharf 1997; Borgani et al. 1999; Schindler 1999). Moreover, no evidence of evolution is found for other cluster properties, such as the iron abundance (out to $z \sim 0.8$ Mushotzky & Loewenstein 1997) and the core radius of the distribution of hot intra-cluster medium (Vikhlinin et al. 1998). All such signs of evidence suggest a low value for the matter density parameter Ω_m (Carlberg et al. 1997b; Fan, Bahcall, & Cen 1997; Henry 1997; Borgani et al. 2000; see Mushotzky 2000 for a review).

However, the validity of these studies relies on our actual understanding of the internal physics of both nearby and distant clusters. In particular, there is evidence that sev-

eral clusters at moderate/distant redshift ($z \sim 0.2$ out to $z \sim 1$) are far from the state of dynamical equilibrium suggesting that present observations are reaching the epoch of cluster assembly. For instance, it is claimed that distant clusters often show discrepancy in determination of mass estimates (e.g., Miralda-Escudé & Babul 1995; Wu & Fang 1996; 1997), where the problems concern, in particular, the cores of clusters (e.g., Allen 1998; Wu, Fang, Xue 1998), and are probably due to the lack of dynamical equilibrium or of spherical symmetry (e.g., Allen, Fabian, & Kneib 1996; Girardi et al. 1997b). Moreover, direct optical and X-ray observations show the strong elongation of some distant clusters (e.g., Gioia et al. 1999).

In this framework, it is worth to analyze the internal dynamics of distant clusters comparing, in particular, the results with those obtained for nearby clusters. Here we focus our attention on the results as they come from the kinematical and spatial analysis of cluster member galaxies.

As for nearby clusters (at redshift $z \lesssim 0.15$), available results are based on very large samples, up to $\gtrsim 100$ clusters, each with several galaxy redshifts available and treated in homogeneous way: the ENACS (ESO Nearby Abell Cluster Survey, Katgert et al. 1998) sample, and compilations collecting ENACS data and other clusters from the literature (den Hartog & Katgert 1996; Fadda et al. 1996, and the following updating by Girardi et al. 1998b – hereafter F96 and G98, respectively). Significant substructures are found for 30–40% of clusters from both the distribution of member galaxies (e.g., Girardi et al. 1997a; Biviano et al. 1997; Solanes, Salvador-Sol’e, and González-Casado 1999) and X-ray analyses (Jones & Forman 1999), with a good one-to-one correspondence between the optical and the X-ray images (Kolokotronis et al. 2000). However, with the exception of strongly

TABLE 1
CLUSTER SAMPLE

Cluster Name	Other Names	<i>N</i>	References
(1)	(2)	(3)	(4)
A115 ^a	ZwCl0053.4+2604	28	1
A140 ^a	EDCC 520	11	2
A222		33	3
A223		28	3
A370		58	4
A520	MS0451.5+0250	27	3
A521		49	5
A665	ZwCl0826.1+6554	41	6
A851	Cl 0939+47	137	4,7
A1300		95	8
A1689		130	9
A2218		53	10
A2390	RXJ2153.6+1741	325	11
A2744	AC118	76	12,13
A3639		14	14
A3854	C52	41	15
A3888	CL22315-3800	98	9
A3889		26	16
AS506 ^a	CL0500-24	29	17
AS910	AC103	88	12,13
AS1077	AC114	103	13,18
CL0017-20 ^a		26	17
CLJ0023+0423	GHO0021+0406	107	19,20
CL0024+16	ZwCl0024.0+1652	134	4,7
CL0053-37		22	16
CL0054-27	J1888.16CL	25	4
CL0303+17	GHO0303+1706	84	4
CL0412-65		24	4
CL0949+44	GHO0949+4408	33	7
CL1447+26		29	4
CL1601+42	GHO1601+4259	101	4,7
CLJ1604+4304	GHO1602+4312	95	19,20
F1637.23TL		19	21
F1652.20CR		20	21
J2175.15TR		19	21
J2175.23C		19	21
MS0015.9+1609	CL0016+1609 HSTJ001831+16207	111	22
MS0302.7+1658	Cl0302+1658	96	23
MS0302.5+1717	Cl0302+1717	43	24
MS0440.5+0204 ^a		56	25
MS0451.6-0305		113	22
MS1008.1-1224		109	26
MS1054.4-0321 ^a		32	27
MS1224.7+2007		54	28
MS1358.4+6245	ZwCl1358.1+6245	281	26
MS1512.4+3647		282	28
MS1621.5+2640		262	23
RXJ1716+67		37	29
1E0657-56 ^a	RASS1 069	32	30
3C206 ^a		15	31
3C295		38	4,7

^a Clusters for which spectral/morphological information is not available.

(1) Zabludoff et al. 1990; (2) Collins et al. 1995; (3) Proust et al. 2000; (4) Dressler et al. 1999; (5) Maurogordato et al. 1999; (6) Oegerle et al. 1991; (7) Dressler & Gunn 1992; (8) Lemonon et al. 1997; (9) Teague et al. 1990; (10) Le Borgne et al. 1992; (11) Yee et al. 1996a; (12) Couch et al. 1998; (13) Couch & Sharples 1987; (14) Garilli et al. 1991; (15) Colless & Hewett 1987; (16) Cappi et al. 1998; (17) Infante et al. 1994; (18) Couch et al. 1994; (19) Lubin et al. 1998b; (20) Postman et al. 1998; (21) Bower et al. 1997; (22) Ellingson et al. 1998; (23) Ellingson et al. 1997; (24) Fabricant et al. 1994; (25) Gioia et al. 1998; (26) Yee et al. 1998; (27) Tran et al. 1999; (28) Abraham et al. 1998; (29) Gioia et al. 1999; (30) Tucker et al. 1998; (31) Ellingson et al. 1989.

Cluster names: “A” for the catalog of Abell et al. (1989) and, in particular, “AS” for the supplementary southern clusters; “AC” and “C” for clusters used by Couch & Newell (1984), and by Colless & Hewett (1987), respectively, taken from the southern extension of the Abell catalog (Abell et al. 1989) in preparation at that time; “EDCC” for the Edinburgh–Durham Cluster Catalog (Lumsden et al. 1992); “F” and “J” for the catalog of Couch et al. (1991); “GHO” for the catalog of Gunn et al. (1986); “HST” for the Hubble Space Telescope Medium Deep Survey cluster sample of Ostrander et al. (1998); “MS” for the Extended Medium Sensitivity Survey (Gioia et al. 1990); “RASS1” for the sample of bright clusters of galaxies in the southern

substructured clusters (e.g., a 10% of bimodal clusters, see Girardi et al. 1997a; G98), most clusters seem not to be far from a global dynamical equilibrium. Finally, galaxy light is a good tracer of dark matter (e.g., Natarajan et al. 1998). The comparison between reliable estimates of velocity dispersions and X-ray temperatures of clusters suggests that the galaxy and hot gas components are not far from energy equipartition per unit mass; the possible discrepancies are likely to require extra-heating sources for poor clusters (e.g., White 1991; Bird, Mushotzky, & Metzler 1995; G98). There is an overall agreement between mass estimates inferred from the analysis of member galaxies and those from X-ray analysis of the hot gas (G98). Other detailed studies concern comparative analyses of different galaxy populations and their use as tracers of the cluster potential (e.g., early- and late-type ones, galaxies with or without emission lines, see, e.g., Biviano et al. 1997; Adami, Biviano, & Mazure 1998).

As for more distant clusters ($z > 0.2$), the possible evolution of member galaxies is well studied (e.g., Butcher & Oemler 1978; Dressler et al. 1997; Abraham et al. 1998), but there are less definitive results on cluster internal dynamics. Most results come from the analysis of the 16 clusters at intermediate redshifts of CNOC (Canadian Network for Observational Cosmology, $0.18 < z < 0.55$; Yee, Ellingson, & Carlberg 1996b) which represent a remarkably homogeneous sample. In particular, as also found in nearby clusters, Lewis et al. (1999) claim for consistency between masses coming from optical and X-ray data, and Carlberg et al. (1997a) find that blue and red galaxies have different distributions in velocity and position. However, the difficulty of obtaining many redshifts in distant clusters has prevented from building larger samples. Rather, several works, concerning one or a small number of clusters, and using different techniques of analysis, can be found in the literature.

The availability of a variety of techniques, already applied to nearby clusters, suggests their application to distant clusters. We thus ensure the homogeneity of our results over a large range of cosmological distances. A homogeneous analysis is in fact fundamental for the understanding of the evolution of cluster properties.

Here, we apply the techniques already used by G98 (cf. also F96) on a sample of 170 nearby clusters (at $z < 0.15$, data from ENACS and other literature) to analyze a collection of 51 distant clusters at $0.15 \lesssim z \lesssim 0.9$.

The paper is organized in the following manner. We shortly describe the data sample and our selection procedure for cluster membership assignment in § 2 and § 3, respectively. We compute internal velocity dispersions and masses for clusters in § 4, with the exception of the three clusters with strong dynamical uncertainties which are discussed in the Appendix A. We compare the “active” and the non “active” galaxies in § 5. We compare our results with those coming from X-ray and weak gravitational lensing analyses in § 6. We give a brief summary of our main results and draw our conclusions in § 7.

Unless otherwise stated, we give errors at the 68% con-

fidence level (hereafter c.l.)

A Hubble constant of $100 h \text{ km s}^{-1} \text{ Mpc}^{-1}$ and a deceleration parameter of $q_0 = 0.5$ are used throughout.

2 THE DATA SAMPLE

We consider 51 clusters at moderate/distant redshift $z > 0.15$ (median $z = 0.33$), each cluster having at least 10 galaxies with available redshift and showing a significant peak in the redshift space. We remark that, due to the difficulty of obtaining redshift data for distant clusters, we relax the requirements already applied to the sample of nearby clusters of G98 ($z < 0.15$, cf. also F96). In particular, we consider also clusters with less than 30 available galaxy redshift, although we never take into account clusters which, after the procedure of the rejection of interlopers, are left with < 5 member galaxies. We relax also other requirements concerning the reliability of the estimate of velocity dispersion, i.e. the requirement of small errors on velocity dispersion ($\lesssim 150 \text{ km s}^{-1}$), and of flat integrated velocity dispersion profile in external cluster regions (cf. § 4.1 for more details).

Cluster data are collected from the literature. In order to achieve sufficiently homogeneous cluster data, the galaxy redshifts in each cluster are usually taken from only one reference source; different sources are used only when the data-sets are proved to be compatible. The data used for each cluster concern galaxy positions, redshifts with the respective errors, and, when available, spectral/morphological information.

Table 1 lists all the 51 clusters considered: in Col. (1) we list the cluster names; in Col. (2) we report other alternative names found in the literature; in Col. (3) the number of galaxies with measured redshift in each cluster field; in Col. (4) the data references.

3 CLUSTER MEMBER SELECTION

In order to select member galaxies, we apply the same procedure as G98 (cf. also F96).

We first use position and velocity information sequentially; then we use the two sets of data combined. In the first two steps we use the adaptive kernel technique by Pisani (1993,1996) as described in the Appendix A of Girardi et al. (1996). The adaptive kernel technique is a nonparametric method for the evaluation of the density probability function underlying an observational discrete data set. For each detected peak, the method gives the corresponding significance and object density, as well as the associate objects.

Firstly, we apply to each cluster field the two-dimensional adaptive kernel analysis to detect clusters which show an obvious bimodality in their projected galaxy distribution: i.e. formed by two significant ($> 99\%$ c.l.) clumps separated by a distance of $\gtrsim 0.5 h^{-1} \text{ Mpc}$. These clumps are then analyzed separately.

Afterwards, we apply the one-dimensional analysis to find the significant peaks in velocity distributions. The

TABLE 2
CLUSTER MEMBERSHIP

Cluster Name	N_p	N_g	N_m	$\langle z \rangle$	Center	
					R.A.(J2000)	δ (J2000)
(1)	(2)	(3)	(4)	(5)	(6)	
A115S	16	13	13	.1958	00:55:59.90	+26:20:08.3
A140	7	7	7	.1600	01:04:31.55	-23:57:46.2
A222	29	27	26	.2138	01:37:33.83	-12:59:21.1
A223	18	18	14	.2119	01:37:56.48	-12:48:33.9
A370	38	37	35	.3744	02:39:51.58	-01:34:12.4
A520	19	18	18	.2000	04:54:14.42	+02:57:14.8
A521	40	37	35	.2474	04:54:09.13	-10:14:25.1
A665	31	26	25	.1806	08:30:46.85	+65:53:52.9
A851	67	65	55	.4061	09:42:58.15	+46:59:34.9
A1300	62	59	53	.3078	11:31:57.69	-19:54:35.2
A1689a	41	38	38	.1837	13:11:31.62	-01:20:58.0
A1689b	16	16	15	.1746	13:11:28.58	-01:20:25.3
A1689ab	57	50	49	.1821	13:11:30.24	-01:20:54.2
A2218	45	43	43	.1761	16:35:51.96	+66:12:19.8
A2390	243	211	200	.2282	21:53:36.80	+17:41:32.2
A2744a	36	36	34	.3014	00:14:21.26	-30:23:49.3
A2744b	27	26	25	.3148	00:14:20.57	-30:24:04.4
A2744ab	63	57	55	.3078	00:14:21.16	-30:23:52.4
A3639	8	8	7	.1480	19:28:18.41	-50:54:28.6
A3854a	21	18	18	.1520	22:17:53.03	-35:46:42.7
A3854b	13	13	9	.1459	22:17:33.97	-35:44:47.1
A3854ab	34	34	30	.1506	22:17:46.50	-35:45:12.3
A3888	81	55	50	.1508	22:34:26.90	-37:43:51.0
A3889a	7	7	7	.2559	22:34:54.47	-30:33:50.5
A3889b	9	9	9	.2495	22:34:49.35	-30:32:13.1
AS506	23	21	21	.3201	05:01:11.85	-24:25:01.5
AS910	56	54	53	.3076	20:57:02.89	-64:40:04.7
AS1077	85	70	63	.3148	22:58:47.14	-34:47:59.8
CL0017-20	20	20	20	.2717	00:19:37.82	-20:26:39.1
CLJ0023+0423a	14	14	5	.8453	00:23:52.69	+04:19:38.3
CLJ0023+0423b	7	7	5	.8273	00:23:53.82	+04:23:16.2
CL0024+16	102	95	73	.3937	00:26:34.79	+17:10:04.8
CL0053-37	20	20	20	.1652	00:55:59.44	-37:32:36.1
CL0054-27	10	9	7	.5604	00:56:56.04	-27:40:31.9
CL0303+17	44	43	29	.4195	03:06:14.13	+17:18:09.0
CL0412-65	7	7	6	.5086	04:12:53.39	-65:51:13.2
CL0949+44a	15	15	14	.3781	09:52:57.50	+43:55:37.0
CL0949+44b	9	9	8	.3493	09:53:01.25	+43:55:22.6
CL1447+26	16	11	5	.3763	14:49:28.78	+26:06:58.3
CL1601+42	57	53	46	.5403	16:03:10.46	+42:45:37.2
CLJ1604+4304	19	14	8	.9018	16:04:25.09	+43:04:11.0
F1637.23TL	8	8	6	.47903	23:59:20.68	-32:17:45.3
F1652.20CR	8	8	6	.4102	04:47:57.66	-20:37:29.6
J2175.15TR	8	8	8	.3948	03:34:20.71	-38:53:54.5
J2175.23C	10	6	5	.4058	03:32:59.30	-39:06:49.7
MS0015.9+1609	63	50	42	.5490	00:18:33.49	+16:26:02.5
MS0302.7+1658	37	33	30	.4248	03:05:31.63	+17:10:12.0
MS0302.5+1717	28	26	24	.4241	03:05:17.92	+17:28:34.4
MS0440.5+0204	32	32	32	.1969	04:43:09.46	+02:10:29.5
MS0451.6-0305	67	46	40	.5403	04:54:11.24	-03:00:45.4
MS1008.1-1224	74	71	65	.3070	10:10:31.76	-12:40:05.4
MS1054.4-0321	32	32	32	.8318	10:56:57.31	-03:37:44.2
MS1224.7+2007	23	23	23	.3253	12:27:18.81	+19:50:26.7
MS1358.4+6245	185	141 ^a	133	.3278	13:59:50.92	+62:30:49.8
MS1512.4+3647	70	46	35	.3711	15:14:16.45	+36:34:57.7
MS1621.5+2640	119	106	88	.4271	16:23:34.52	+26:34:17.1
RXJ1716+67	37	32	19	.8073	17:16:48.92	+67:08:21.1
1E0657-56	14	12	12	.2966	06:58:37.83	-55:56:56.0
3C206	7	7	7	.1980	08:39:50.10	-12:14:32.2
3C295	21	21	15	.4591	14:11:21.54	+52:11:54.6

3.1 Results for Specific Clusters

main cluster body is naturally identified as the highest significant peak. All galaxies not belonging to this peak are rejected as non cluster members. F96 and G98 required that peaks are significant at the 99% c.l. and, for clusters with secondary peaks, they assumed that the peaks are separable when their overlapping is $\leq 20\%$ and their velocity separation is $\Delta v \geq 1000 \text{ km s}^{-1}$ (here, we consider 1000 km s^{-1} in the appropriate cluster rest-frame). In dealing with distant clusters, we apply the peak analysis to very poor samples, so obtaining small peak probability: in a few fields we identify clusters with the highest peak having significance $< 99\%$ (but always $> 95\%$).

The combination of position and velocity information, represented by plots of velocity vs. clustercentric distance, reveals the presence of surviving interlopers (e.g., Kent & Gunn 1982; Regös & Geller 1989). To identify these interlopers in the above-detected systems we apply the procedure of the “shifting gapper” by F96. We apply the fixed gap method to a bin shifting along the distance from the cluster center. According to F96 prescriptions, we use a gap of $\geq 1000 \text{ km s}^{-1}$ (in the cluster rest-frame) and a bin of $0.4 h^{-1} \text{ Mpc}$, or large enough to include 15 galaxies. As for very poor distant clusters (with less than 15 members), we reject galaxies that are too far in velocity from the main body of galaxies of the whole cluster (considering a somewhat larger gap, cf. § 3.1 for details).

When early- and late-galaxy type populations showed different mean and variance in the velocity distribution, Girardi et al. (1996) retained only the early population as better tracer of the cluster potential. Similarly, when only spectral information was available, F96 applied the same procedure by rejecting emission line galaxies (hereafter ELGs, while NELGs indicate galaxies without emission lines). Indeed there is evidence that ELGs lead to too high estimates of internal velocity dispersion (e.g., Koranyi & Geller 2000) and that they could be not in dynamical equilibrium within the cluster potential (Biviano et al. 1997). For distant clusters, galaxy morphologies are generally not available, but spectral type and/or color give information about the presence of some nuclear galaxy activity or strong star formation. For the 43 out of 51 cluster samples with available information, we reject the likely “active” galaxies (hereafter AGs), i.e. galaxies having a strong star formation activity and/or signs of nuclear activity (see our classification in § 3.2).

Table 2 lists the results of the member selection procedure (cf. § 3.1 for details on some specific clusters). In Col. (1) we list the system name, i.e. the name of the parent cluster with possible indication of the peak (e.g. A1689a and A1689b); in Col. (2) the number of galaxies found by the adaptive kernel method in each peak, N_p ; in Col. (3) the number of galaxies left after the “shifting gapper”, N_g ; in Col. (4) the number of member galaxies after the rejection of the AGs, N_m , and used to compute the mean redshift determined via the biweight estimator (Beers, Flynn, & Gebhardt 1990), and the cluster center as determined via the two-dimensional adaptive kernel (in Cols. (5) and (6), respectively).

According to our analysis of galaxy distribution, we find indication for bimodality only in the case of A115 (cf. also Forman et al. 1981; Beers, Geller, & Huchra 1983). Moreover, we consider only the Southern peak, A115S, since the Northern peak has too few galaxies to survive to the whole procedure of member selection.

According to our analysis of cluster velocity distributions, out of the 51 cluster fields here analyzed, we find 51 well-separated peaks (45 from 45 one-peaked fields and six from three two-peaked fields) and three fields with two strongly superimposed peaks.

The three fields showing two separable peaks are A3889, CL0949+44 (cf. also Dressler & Gunn 1992), and CLJ0023+0423. In particular, the field of the CLJ0023+0423 cluster shows a complex structure in the velocity distribution, containing a system of four peaks strongly superimposed; however, when reanalyzing only galaxies belonging to this system, we find two peaks. These peaks corresponds to those found by Lubin, Postman, & Oke (1998a, CLJ0023+0423 “A” and “B” instead of our “b” and “a”).

The cluster fields for which the peak separation is not secured at a high c.l. are: A1689 (cf. also Girardi et al. 1997), A2744, and A3854. The strongly overlapped peaks could indicate the presence of substructures in a single system and, in this case, the dynamics of these clusters is strongly uncertain; therefore we consider both the case with the two peaks disjointed or together (e.g., A1689a, A1689b, and A1689ab), cf. the Appendix A for other details.

As for very poor distant clusters (with less than 15 galaxies), the procedure of the “shifting gapper”, which works with a gap of 1000 km s^{-1} in a shifting bin considering at least 15 galaxies, cannot be applied. In these cases we reject galaxies that are too far in velocity from the main body of galaxies of the whole cluster rather than in a shifting bin. Moreover, we adopt a slightly larger gap since the suitable size of the gap increases with the available statistics (cf. the density-gap by Adami et al. 1998). We reject one galaxy in CL0054-27, one galaxy in J2175.23C, and two galaxies in 1E0657-56, where the gap is $\gtrsim 2000 \text{ km s}^{-1}$. The situation is less obvious for other two galaxies in CL0054-27 and other three galaxies in J2175.23C, where the respective gaps are $\sim 1150 \text{ km s}^{-1}$, $\sim 1300 \text{ km s}^{-1}$, respectively. For CL0054-27, the two uncertain members are close to the center and we decide to retain them. Instead, for J2175.23C, we decide to reject the three uncertain members, which are connected to the main body of galaxies only thanks to the presence of an AG. Moreover, two of the uncertain members are AGs, and the other uncertain member would result the most distant galaxy from the cluster center. Monte Carlo simulations performed in § 4.4 show that, in the case of poor statistics, a fixed gap of $\sim 1250 \text{ km s}^{-1}$ allows us to well recover, on average, the estimate of velocity dispersion.

As for the combined analysis of position and velocity in-

formation, the plot of rest-frame velocity versus projected clustercentric distance of MS1358.4+6245 shows the existence of a close system corresponding to a southern group (cf. Carlberg et al. 1996). We exclude this group rejecting all galaxies outside $1.2 h^{-1} Mpc$ (cf. also Borgani et al. 1999).

3.2 Classification of “Active Galaxies”

As for our classification of AGs, in several cluster samples only main galaxy spectral features are reported. In these cases we classify as “active” galaxies to be rejected those where the presence of emission lines is reported. For other clusters, where more detailed information is given, we always reject galaxies with very strong emission lines or classified as starburst or AGN: in the following we describe the classification adopted for these specific studies.

As for the data by Postman, Lubin, & Oke (1998), we reject galaxies with the presence of a $[OII]$ line with an equivalent width of $EW[OII] \gtrsim 15 \text{ \AA}$, which corresponds, according to the authors, to an active, star forming galaxy.

As for the data by Dressler et al. (1999), we consider as AGs those galaxies classified from their spectra as “e(a)” (with strong Balmer absorption plus $[OII]$ emission), “e(n)” (having AGN spectra), or “e(b)” (with very strong $[OII]$ emission, possibly starburst galaxies). As for data by Dressler & Gunn (1992), “active” galaxies are those classified with “e” (with emission lines, usually $[OII]$ or $[OIII]$) or “n” (with very strong emission, likely due to AGN).

As for the CNOC clusters (Yee et al. 1996a; Ellingson et al. 1997; Abraham et al. 1998; Ellingson et al. 1998; Yee et al. 1998), we consider as AGs those galaxies classified from their spectra with “5” (with emission lines, likely irregular galaxies) or “6” (likely AGN/QSO).

Finally, we also consider as AGs those galaxies labeled “starburst” by Couch et al. (1998, and previous works by Couch & Sharples 1987 and Couch et al. 1994), which are characterized by blue colors and emission-filled $H\delta$ lines.

4 ANALYSIS OF CLUSTER INTERNAL DYNAMICS

The analysis of the three clusters which show strongly superimposed peaks (A1689, A2744, and A3854) is postponed to the Appendix A. In the following sections we analyze the 45 cluster fields which show only one peak in their velocity distribution and the three cluster fields which show two separable peaks for a total of 51 well-defined systems (cf. § 3.1). This sample can be compared to that of 160 well-separated peaks for nearby clusters of G98. We remark that, on average, the distant clusters are less well sampled as for both the number of cluster members (median $N_m = 21$ vs. 39), and the spatial extension R_{max} , which is the clustercentric distance of the most distant galaxy from the cluster center (median $R_{max} = 0.64$ vs. $1.45 h^{-1} Mpc$). Throughout this analysis we apply homogeneous procedures already used by G98 (cf. also

F96).

4.1 Velocity Dispersions

We estimate the “robust” velocity dispersion line-of-sight, σ_v , by using the biweight and the gapper estimators when the galaxy number is larger and smaller than 15, respectively (cf. ROSTAT routines – see Beers et al. 1990), and applying the relativistic correction and the usual correction for velocity errors (Danese, De Zotti, & di Tullio 1980). In particular, for a few cases where the velocity error is not available, we assume a typical velocity error of $300 km s^{-1}$. When the correction for velocity errors leads to a negative value of σ_v , we list $\sigma_v = 0$.

Following F96 (cf. also Girardi et al. 1996) we analyze the “integral” velocity dispersion profile (hereafter VDP), where the dispersion at a given (projected) radius is evaluated by using all the galaxies within that radius, i.e. $\sigma_v(< R)$. The VDPs allow to check the robustness of σ_v estimate. In particular, although the presence of velocity anisotropy in galaxy orbits can strongly influence the value of σ_v computed for the central cluster region, it does not affect the value of the σ_v computed for the whole cluster (e.g., Merritt 1988). The VDPs of nearby clusters show strongly increasing or decreasing behaviors in the central cluster regions, but they are flattening out in the external regions (beyond $\sim 1 h^{-1} Mpc$, cf. also den Hartog & Katgert 1996) suggesting that in such regions they are no longer affected by velocity anisotropies. Thus, while the σ_v -values computed for the central cluster region could be a very poor estimate of the depth of cluster potential wells, one can reasonably adopt the σ_v value computed by taking all the galaxies within the radius at which the VDP becomes roughly constant. As for the distant clusters we analyze, when the data are good enough, the VDPs show a behavior similar to that of nearby clusters (cf. Figure 1). Unfortunately, distant clusters suffer for the poor sampling, and also for the small spatial extension of the sampled cluster region. Indeed, the strongly decreasing VDP in the external sampled regions of some clusters (maybe the striking cases are AS506, CL0017-20, CL0054-27, 3C295) suggests that the correct estimates of velocity dispersions could be smaller than those, σ_v , we can estimate with present data; therefore, in these cases, σ_v should be better interpreted as an upper limit (see also some cases in F96; these cases were then not considered in G98). In other cases, when the member galaxies are too few, the analysis of VDPs does not allow any conclusion.

In Table 3 we report the value of σ_v computed considering all member galaxies. However, we make a note for the clusters which do not share the requirements for the nearby clusters of F96 and G98, i.e.: with an original number of galaxies in the field smaller than 30; with a peak in the velocity distribution less significant than 99%; with an error on σ_v larger than $150 km s^{-1}$; with a VDP which is poorly defined or without a flat behavior in the external cluster regions.

After fixing the cosmological background, the theory of a spherical model for nonlinear collapse allows to recover

the value of the radius of virialization, R_{vir} , within which the cluster can be considered not far from a status of dynamical equilibrium. The relation between the density of a collapsed (virialized) region and the cosmological density is $\rho_{vir} = 18\pi^2 \rho_{cr} = 18\pi^2 \times 3H^2/8\pi G$ (for a $\Omega_m = 1$ universe). As a first approximation, the mass contained within R_{vir} , $M_{vir} = (4\pi/3) \cdot R_{vir}^3 \rho_{vir}$, is given by the virial estimate $(3\pi/2) \cdot (\sigma_v^2 R_{vir} f_\Sigma / G)$, where f_Σ depends on the details of galaxy spatial distribution (e.g., G98). Therefore $R_{vir}^2 = \sigma_v^2 f_\Sigma / (6\pi H^2)$, where $H = 100 \cdot h(1+z)^{3/2}$. For nearby clusters G98 give a first rough estimate of

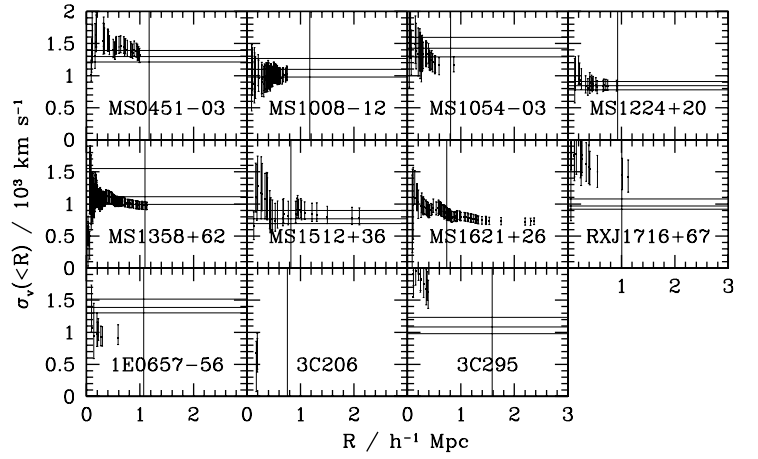
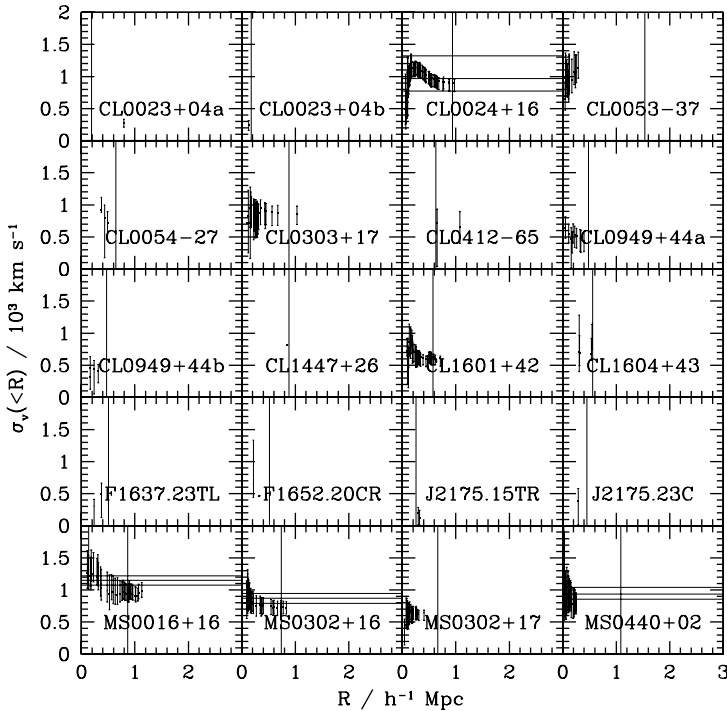
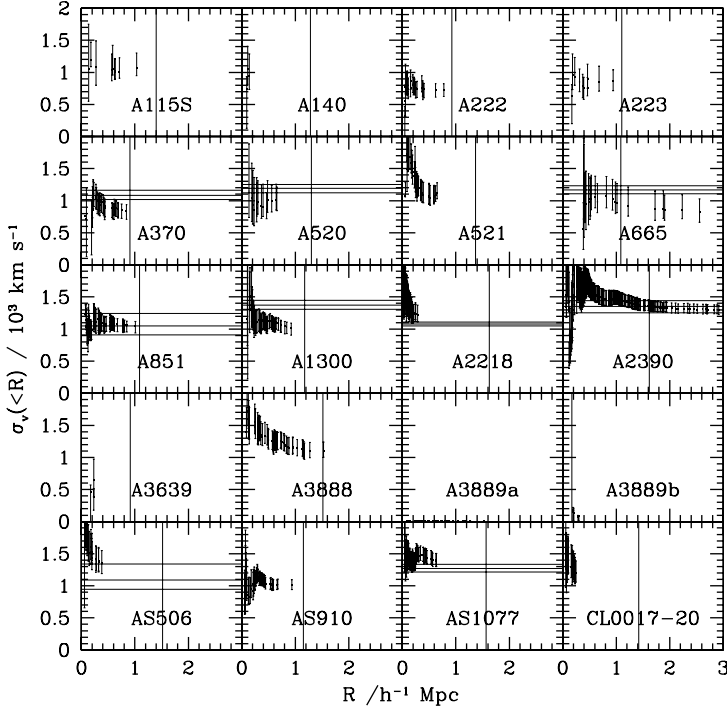


Fig. 1.— Integrated line-of-sight velocity dispersion profiles $\sigma_v(<R)$, where the dispersion at a given (projected) radius from the cluster center is estimated by considering all galaxies within that radius. The bootstrap error bands at the 68% c.l. are shown. The horizontal lines represent X-ray temperature with the respective errors (cf. Table 4) transformed in σ_v imposing $\beta_{spec} = 1$ (where $\beta_{spec} = \sigma_v^2 / (kT / \mu m_p)$, with μ the mean molecular weight and m_p the proton mass). The vertical faint lines indicate the virialized region within R_{vir} .

$R_{vir} \sim 0.002 \cdot \sigma_v (km^{-1}s h^{-1} Mpc)$. A following re-estimate of Girardi et al. (1998a) suggests rather a scaling factor of 0.0017. Since we find that distant clusters have a galaxy distribution similar to that of nearby ones (see in the following), we adopt here the same scaling relation with σ_v :

$$R_{vir} \sim 0.0017 \cdot \sigma_v / (1+z)^{3/2} (km^{-1}s h^{-1} Mpc) \quad (1)$$

introducing only the scaling with redshift (cf. also Carlberg et al. 1997c for a similar relation).

4.2 Galaxy Distribution

As for the study of the spatial distribution of galaxies within distant clusters, following G98 (cf. also Girardi et al. 1995; Adami et al. 1998) we fit the galaxy surface density of each cluster to a King-like distribution (comparable to the β -profile in fitting the distribution of hot diffuse intracluster gas):

$$\Sigma(R) = \frac{\Sigma_0}{[1 + (R/R_c)^2]^\alpha}, \quad (2)$$

where R_c is the core radius and α is the parameter which describes the galaxy distribution in external regions ($\alpha = 1$ corresponds to the classical King distribution). This surface density profile corresponds to a galaxy volume-density $\rho = \rho_0 / [1 + (r/R_c)^2]^{3\beta_{fit,gal}/2}$, with $\beta_{fit,gal} = (2\alpha + 1)/3$, i.e. $\rho(r) \propto r^{-3\beta_{fit,gal}}$ for $r \gg R_c$. We perform the fit through the Maximum Likelihood technique, allowing R_c and α to vary from 0.01 to $1 h^{-1} Mpc$ and from 0.5 to 1.5, respectively.

To avoid possible effects due to the non circular sampling of clusters, by visual inspection of the original sampled region of each cluster we extract the largest circular region, with center as in Table 2, there inscribed. We perform the fit within this circular cluster region whose radius

we define as $R_{max,c}$. We consider only the 30 clusters with at least ten member galaxies within $R_{max,c}$ and, in particular, a subsample of 13 clusters with $R_{max,c}/R_{vir} > 0.5$.

The median value of α , with the respective errors at the 90% c.l., is $= 0.63_{-0.08}^{+0.08}$, and 0.67 is found when we consider only the 13 clusters with a large sampled radius. This value agrees with $\alpha = 0.70_{-0.03}^{+0.08}$ found for nearby clusters, and corresponds to a $\beta_{fit,gal} \sim 0.8$, i.e. to a volume galaxy–density $\rho \propto r^{-2.4}$. After fixing $\alpha = 0.7$, we again fit the galaxy distribution of each cluster, obtaining a median value of $R_c = 0.045_{-0.015}^{+0.005} h^{-1} Mpc$ (and $0.05 h^{-1} Mpc$ for the well-sampled 13 clusters). Thus, in our cluster sample, the typical value of R_c (and $R_{vir}/R_c \sim 20$) is again in agreement with that found in nearby clusters where $R_c = 0.05 \pm 0.01 h^{-1} Mpc$. Hereafter, we assume the above King–modified distribution, with the same parameters of nearby clusters, i.e. $\alpha = 0.7$ and $R_c = 0.05 h^{-1} Mpc$, for all clusters of our sample.

4.3 Virial Masses and Velocity Anisotropies

Assuming that clusters are spherical, non rotating systems, and that the internal mass distribution follows galaxy distribution, cluster masses can be computed throughout the virial theorem (e.g., Limber & Mathieus 1960; The & White 1986) as:

$$M = M_V - C = \frac{3\pi}{2} \cdot \frac{\sigma_v^2 R_{PV}}{G}, \quad (3)$$

where the projected virial radius,

$$R_{PV} = N(N-1)/(\sum_{i>j} R_{ij}^{-1}), \quad (4)$$

describes the galaxy distribution and is computed from projected mutual galaxy distances, R_{ij} ; C is the surface term correction to the standard virial mass M_V and it is due to the fact that the system is not entirely enclosed in the observational sample (cf. also Carlberg et al. 1996; G98).

Following G98 we want to estimate cluster masses contained within the radius of virialization, R_{vir} . In fact, clusters cannot be assumed in dynamical equilibrium outside R_{vir} and considering small cluster regions leads to unreliable measures of the potential (σ_v could be strongly affected by velocity anisotropies) and of the surface term correction (Koranyi & Geller 2000).

Only few distant clusters are sampled out to R_{vir} . As for σ_v , the above analysis of the VDP give indications about its reliability, i.e. VDPs which are flat in the external cluster regions will give reliable estimates of σ_v even when clusters are not sampled out to R_{vir} . As for R_{PV} , which describes the galaxy spatial distribution, it can be recovered in an alternative theoretical way from the knowledge of the parameters of the King–like distribution (Girardi et al. 1996; see also G98 for a simple analytical approximation in the case of $\alpha = 0.7$ and $R_c/R_{vir} = 0.05$). This procedure allows to compute R_{PV} at each cluster radius and, in particular, we compute R_{PV} at R_{vir} , which is needed in the computation of the mass within R_{vir} . By using well-sampled nearby clusters G98 verified the reliability of this

alternative estimate and evaluated the typical error introduced by the use of the average King–like parameters of the sample ($\sim 0.2 h^{-1} Mpc$, corresponding to about 25% of R_{PV}).

The computation of the C correction at the boundary radius, b ,

$$C = M_V \cdot 4\pi b^3 \frac{\rho(b)}{\int_0^b 4\pi r^2 \rho dr} [\sigma_r(b)/\sigma(<b)]^2, \quad (5)$$

requires the knowledge of the velocity anisotropy of galaxy orbits. In fact, $\sigma_r(b)$ is the radial component of the velocity dispersion $\sigma(b)$, while $\sigma(<b)$ refers to the integrated velocity dispersion within b ; here $b = R_{vir}$. Having assumed that in clusters the mass distribution follows the galaxy distribution, one can use the Jeans equation to estimate velocity anisotropies from the data, i.e. from the (differential) profile of the line-of-sight velocity dispersion, $\sigma_v(R)$. Unfortunately, this profile requires a large number of galaxies and we can compute it only by combining together the data of many clusters, without preserving cluster individuality.

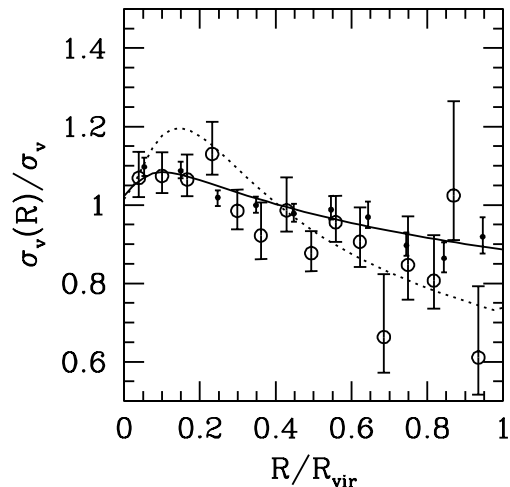


Fig. 2.— The (normalized) line-of-sight velocity dispersion, $\sigma_v(R)$, as a function of the (normalized) projected distance from the cluster center. The points represent data combined from all clusters and binned in equispacial intervals. We give the robust estimates of velocity dispersion and the respective bootstrap errors. We give the results for distant clusters (open circles) and for nearby clusters taken from Girardi et al. (1998b, filled circles). The solid and dotted line represent the models for isotropic and moderate radial orbits of galaxies, respectively (see text).

For both nearby and distant clusters, Figure 2 shows the observational $\sigma_v(R)$ computed by combining together the galaxies of all clusters, i.e. by normalizing distances to R_{vir} and velocities, relative to the mean cluster velocity, to the observed global velocity dispersion σ_v . For nearby

TABLE 3
DYNAMICAL PROPERTIES

Name	N_m	R_{max} $h^{-1} Mpc$	σ_v $km s^{-1}$	R_{vir} $h^{-1} Mpc$	R_{PV}	T	M_V $h^{-1} 10^{14} M_\odot$	M
(1)	(2)	(3)	(4)	(5)	(6)	(7)	(8)	(9)
A115S ^{a,c}	13	0.91	1074 ⁺²⁰⁸ ₋₁₂₁	1.40	0.98	B	12.40 ^{+5.72} _{-4.17}	9.98 ^{+4.60} _{-3.36}
A140 ^{a,c,d}	7	0.13	941 ⁺³⁶⁹ ₋₂₅₁	1.28	0.91	-	8.86 ^{+7.29} _{-5.22}	7.11 ^{+5.85} _{-4.19}
A222	26	0.75	730 ⁺¹⁰² ₋₉₆	0.93	0.70	A	4.08 ^{+1.53} _{-1.48}	2.23 ^{+0.84} _{-0.81}
A223 ^{a,c}	14	0.81	868 ⁺¹⁸⁶ ₋₁₂₄	1.11	0.81	A	6.67 ^{+3.31} _{-2.53}	3.73 ^{+1.85} _{-1.42}
A370	35	0.81	859 ⁺¹¹⁸ ₋₁₁₂	0.91	0.68	C	5.53 ^{+2.06} _{-2.00}	4.75 ^{+1.76} _{-1.72}
A520 ^{a,c}	18	0.60	1005 ⁺²²⁹ ₋₁₃₂	1.30	0.92	C	10.23 ^{+5.32} _{-3.71}	8.85 ^{+4.60} _{-3.21}
A521	35	0.64	1123 ⁺¹⁴⁶ ₋₁₀₂	1.37	0.97	B	13.35 ^{+4.82} _{-4.13}	10.74 ^{+3.87} _{-3.32}
A665 ^c	25	2.41	821 ⁺²³³ ₋₁₃₀	1.09	0.80	-	5.88 ^{+3.65} _{-2.37}	4.70 ^{+2.92} _{-1.90}
A851	55	1.01	1067 ⁺⁸⁹ ₋₉₆	1.09	0.80	C	9.94 ^{+2.99} _{-3.06}	8.57 ^{+2.58} _{-2.64}
A1300	53	0.86	1034 ⁺⁸⁹ ₋₁₀₄	1.18	0.85	B	9.95 ^{+3.02} _{-3.19}	7.97 ^{+2.42} _{-2.56}
A2218	43	0.32	1222 ⁺¹⁴⁷ ₋₁₀₉	1.63	1.12	-	18.27 ^{+6.34} _{-5.61}	14.77 ^{+5.12} _{-4.54}
A2390	200	3.07	1294 ⁺⁷⁶ ₋₆₇	1.62	1.11	A	20.35 ^{+5.62} _{-5.51}	11.79 ^{+3.26} _{-3.19}
A3639 ^{a,c,d}	7	0.23	659 ⁺³⁶⁷ ₋₂₁₆	0.91	0.69	C	3.27 ^{+3.73} _{-2.29}	2.81 ^{+3.20} _{-1.97}
A3888	50	1.44	1102 ⁺¹³⁷ ₋₁₀₇	1.52	1.05	A	14.00 ^{+4.94} _{-4.43}	8.07 ^{+2.85} _{-2.56}
A3889a ^{a,b}	7	0.40	0	-	-	-	-	-
A3889b ^{a,b}	9	0.26	138 ⁺²⁵ ₋₁₃₂	0.17	0.17	-	0.04 ^{+0.02} _{-0.07}	0.02 ^{+0.01} _{-0.05}
AS506 ^{a,c,e}	21	0.38	1356 ⁺²⁰⁴ ₋₁₅₀	1.52	1.05	B	21.23 ^{+8.30} _{-7.09}	17.13 ^{+6.70} _{-5.72}
AS910	53	0.80	1010 ⁺⁹⁴ ₋₇₃	1.15	0.83	B	9.32 ^{+2.90} _{-2.69}	7.45 ^{+2.32} _{-2.15}
AS1077	63	0.67	1388 ⁺¹²⁸ ₋₇₁	1.57	1.08	B	22.79 ^{+7.08} _{-6.16}	18.41 ^{+5.72} _{-4.97}
CL0017-20 ^{a,c,e}	20	0.23	1197 ⁺²²² ₋₁₂₅	1.42	0.99	-	15.62 ^{+6.99} _{-5.09}	12.58 ^{+5.63} _{-4.10}
CLJ0023+0423a ^d	5	0.48	283 ⁺⁵³ ₋₁₇	0.19	0.19	-	0.17 ^{+0.07} _{-0.05}	0.11 ^{+0.05} _{-0.03}
CLJ0023+0423b ^{b,d}	5	0.12	253 ⁺¹³⁵ ₋₁₇	0.17	0.17	-	0.12 ^{+0.13} _{-0.03}	0.08 ^{+0.09} _{-0.02}
CL0024+16	73	1.03	911 ⁺⁸¹ ₋₁₀₇	0.94	0.71	A	6.42 ^{+1.97} _{-2.20}	3.53 ^{+1.08} _{-1.21}
CL0053-37 ^{a,c}	20	0.23	1136 ⁺²⁵⁹ ₋₁₆₇	1.54	1.06	-	15.03 ^{+7.81} _{-5.80}	12.13 ^{+6.31} _{-4.68}
CL0054-27 ^{a,c,e}	7	0.46	742 ⁺⁵⁹⁹ ₋₁₄₇	0.65	0.52	A	3.12 ^{+5.10} _{-1.46}	1.62 ^{+2.64} _{-0.76}
CL0303+17	29	1.04	876 ⁺¹⁴⁴ ₋₁₄₀	0.88	0.67	B	5.62 ^{+2.32} _{-2.28}	4.45 ^{+1.84} _{-1.81}
CL0412-65 ^{a,c,d}	6	1.04	681 ⁺²⁵⁶ ₋₁₈₅	0.62	0.50	-	2.55 ^{+2.02} _{-1.53}	1.99 ^{+1.58} _{-1.19}
CL0949+44a	14	0.40	458 ⁺¹³⁴ ₋₁₃₁	0.48	0.41	A	0.93 ^{+0.59} _{-0.58}	0.45 ^{+0.29} _{-0.28}
CL0949+44b	8	0.35	434 ⁺¹¹¹ ₋₉₃	0.47	0.40	-	0.82 ^{+0.47} _{-0.41}	0.63 ^{+0.36} _{-0.31}
CL1447+26 ^{a,c,d}	5	0.67	838 ⁺¹⁶³ ₋₁	0.88	0.67	-	5.15 ^{+2.38} _{-1.29}	4.08 ^{+1.89} _{-1.02}
CL1601+42	46	0.62	646 ⁺⁸⁴ ₋₈₇	0.57	0.47	C	2.14 ^{+0.77} _{-0.79}	1.81 ^{+0.65} _{-0.67}
CLJ1604+4304 ^c	8	0.36	858 ⁺²⁷⁷ ₋₈₃	0.56	0.46	-	3.68 ^{+2.55} _{-1.16}	2.85 ^{+1.97} _{-0.90}
F1637.23TL ^{a,c,d}	6	0.35	538 ⁺¹⁰⁶ ₋₃₆₇	0.51	0.42	-	1.34 ^{+0.63} _{-1.87}	1.03 ^{+0.48} _{-1.43}
F1652.20CR ^{a,b,c,d}	6	0.25	510 ⁺⁵¹¹ ₋₅₁₁	0.52	0.43	-	1.23 ^{+2.48} _{-2.48}	0.94 ^{+1.91} _{-1.91}
J2175.15TR ^{a,b,c,d}	8	0.36	246 ⁺⁷⁹ ₋₂₃₉	0.25	0.24	-	0.16 ^{+0.11} _{-0.31}	0.11 ^{+0.08} _{-0.22}
J2175.23C ^{a,c,d}	5	0.29	443 ⁺¹⁷⁷ ₋₄₃₀	0.45	0.38	-	0.83 ^{+0.69} _{-1.62}	0.63 ^{+0.53} _{-1.23}
MS0015.9+1609	42	1.14	984 ⁺¹³⁰ ₋₉₅	0.87	0.66	A	7.00 ^{+2.55} _{-2.21}	3.80 ^{+1.38} _{-1.20}
MS0302.7+1658	30	0.86	735 ⁺¹⁰⁹ ₋₈₀	0.73	0.58	A	3.40 ^{+1.32} _{-1.13}	1.80 ^{+0.70} _{-0.60}
MS0302.5+1717	24	0.41	664 ⁺⁶⁷ ₋₇₇	0.66	0.53	C	2.56 ^{+0.82} _{-0.87}	2.17 ^{+0.70} _{-0.74}
MS0440.5+0204	32	0.23	838 ⁺¹³¹ ₋₁₃₉	10.09	0.80	B	6.13 ^{+2.45} _{-2.55}	4.90 ^{+1.96} _{-2.08}
MS0451.6-0305	40	0.99	1317 ⁺¹²² ₋₁₀₃	1.17	0.85	A	16.10 ^{+5.01} _{-4.75}	9.06 ^{+2.82} _{-2.67}
MS1008.1-1224	65	0.77	1033 ⁺¹¹⁵ ₋₁₀₅	1.18	0.85	C	9.93 ^{+3.33} _{-3.20}	8.58 ^{+2.87} _{-2.76}
MS1054.4-0321	32	0.72	1178 ⁺¹³⁹ ₋₁₁₃	0.81	0.62	A	9.46 ^{+3.25} _{-2.98}	5.08 ^{+1.75} _{-1.60}
MS1224.7+2007	23	0.86	837 ⁺¹⁰⁰ ₋₈₃	0.93	0.70	A	5.38 ^{+1.86} _{-1.72}	2.95 ^{+1.02} _{-0.94}
MS1358.4+6245	133	1.16	985 ⁺⁵⁸ ₋₆₂	10.09	0.80	B	8.51 ^{+2.35} _{-2.38}	6.80 ^{+1.88} _{-1.90}
MS1512.4+3647	35	2.20	776 ⁺¹⁷² ₋₁₀₃	0.82	0.63	C	4.16 ^{+2.12} _{-1.52}	3.56 ^{+1.81} _{-1.30}
MS1621.5+2640	88	2.51	735 ⁺⁵³ ₋₅₃	0.73	0.57	A	3.40 ^{+0.98} _{-0.98}	1.80 ^{+0.52} _{-0.52}
RXJ1716+67 ^c	19	1.03	1445 ⁺²⁸⁸ ₋₂₁₈	1.01	0.75	A	17.17 ^{+8.08} _{-6.73}	9.51 ^{+4.47} _{-3.73}
1E0657-56	12	0.59	926 ⁺¹⁷⁸ ₋₁₀₄	10.07	0.78	B	7.36 ^{+3.38} _{-2.47}	5.87 ^{+2.69} _{-1.97}
3C206 ^{a,c,d}	7	0.22	585 ⁺⁵⁷⁴ ₋₁₅₅	0.76	0.59	-	2.21 ^{+4.38} _{-1.30}	1.74 ^{+3.45} _{-1.02}
3C295 ^{c,e}	15	0.36	1642 ⁺²²⁴ ₋₁₈₇	1.58	1.09	B	32.22 ^{+11.92} _{-10.90}	26.03 ^{+9.63} _{-8.80}

^a Clusters having in their field less than 30 galaxies with available redshift (cf. Table 1).

^b Clusters with a peak in the velocity distribution less significant than 99%.

^c Clusters with an error on σ_v of $\gtrsim 150 km s^{-1}$.

^d Clusters with a VDP which is poorly defined.

^e Clusters with a VDP which is without a flat behavior in the external cluster regions: the strong decreasing suggests that the estimates of σ_v , M_V , and M are better interpreted as upper limits (see text).

clusters the observational profile is well described by a theoretical profile obtained by the Jeans equation, assuming that velocities are isotropic, i.e. that the tangential and radial components of velocity dispersion are equal (i.e., the velocity anisotropy parameter $\mathcal{A} = 1 - \sigma_\theta^2(r)/\sigma_r^2(r) = 0$). For distant clusters this model is less satisfactory, but cannot be rejected being acceptable at the $\sim 15\%$ c.l. (according to the χ^2 probability).

In order to give C -corrections more appropriate to each individual cluster G98 used a profile indicator, I_p , which is the ratio between $\sigma_v(< 0.2 \times R_{vir})$, the line-of-sight velocity dispersion computed by considering the galaxies within the central cluster region of radius $R = 0.2 \times R_{vir}$, and the global σ_v . According to the values of this parameter, they divided clusters in three classes containing the same number of clusters: “A” clusters with a decreasing profile ($I_p > 1.16$), “C” clusters with a increasing profile ($I_p < 0.97$), and an intermediate class “B” of clusters with very flat profiles ($0.97 < I_p < 1.16$). Each of the three types of profiles can be explained by models with a different kind of anisotropy, i.e. radial, isotropic, and circular orbits in the case of A, B, and C clusters, respectively, requiring different values of $[\sigma_r(R_{vir})/\sigma(< R_{vir})]^2$, cf. G98. We can define 14, 11, and 8 clusters of class A, B, and C, respectively, and for each class we use the respective $[\sigma_r(R_{vir})/\sigma(< R_{vir})]^2$ given by G98 to determine the C -corrections. The median values of the relative corrections C/M_V are 45%, 20%, and 14% for A, B, and C clusters, respectively. For 18 clusters we cannot define the kind of profile and we assume the intermediate one. The median correction on the whole sample is then $C/M_V \sim 21\%$, very similar to that found by G98 for nearby clusters and to that suggested by Carlberg et al. (1997c) for CNOC clusters.

In Table 3 we list the results of the cluster dynamical analysis: the number of cluster members as taken from Table 2, N_m (Col. 2); the clustercentric distance of the most distant galaxy from the cluster center, R_{max} (Col. 3); the global line-of-sight velocity dispersion σ_v with the respective bootstrap errors (Col. 4); the radius which defines the region of virialization, R_{vir} (Col. 5); the projected virial radius, R_{PV} , computed at R_{vir} (Col. 6); the cluster type according to their velocity dispersion profile, T (Col. 7); the estimate of cluster mass contained within R_{vir} as determined from the standard virial theorem, M_V , and after the pressure surface term correction, M (Cols. 8 and 9, respectively). The errors on M_V take into account of the errors on σ_v and the above quoted error of 25% on R_{PV} . The percent errors on M_{CV} are the same as for M_V , i.e. we neglect uncertainties on C -correction.

There are some possible suggestions that galaxy orbits in distant clusters have a somewhat more radial velocity anisotropy than those in nearby clusters. Figure 2 shows that the velocity dispersion profile for distant clusters seems less flat than that of nearby clusters. Indeed, according to the available data for distant clusters, also models with moderate radial orbits, i.e. $\mathcal{A} = r^2/(r^2 + r_a^2)$ with $r_a = 0.25 \times R_{vir}$, can be acceptable (at the $\sim 4\%$

c.l.). Moreover, the distant clusters with strongly decreasing profiles (type A) are many more than clusters with increasing profiles (type C), while, for definition, the number of A and C types are equal among nearby clusters. However, we verify that there is no significant difference between the combined profiles of distant and nearby clusters, and that distant and nearby clusters are not different according to the median value of the profile parameter I_p . Therefore, with present data, we conclude that the possible evidence of a larger amount of radial velocity anisotropies in galaxy orbits of more distant clusters is not significant.

4.4 Robustness of the Results

Here we address the effects of the poor sampling on our results, in particular on our estimates of velocity dispersions.

In order to check the effects of the small number of redshifts we perform Monte Carlo simulations by randomly undersampling the 20 cluster fields having more than 50 galaxies and only one peak in the velocity distribution. Since our random undersampling does not consider other parameters like the proximity to the cluster center and the galaxy color, the following results should be considered as conservative.

For each of the 20 cluster fields we perform 500 random simulations extracting ten galaxies each time (the lowest limit in our sample). Then we apply the whole procedure of member selection, i.e. the detection of a significant peak in the velocity distribution via the adaptive kernel method, the application of the fixed gap to the remaining galaxies, and finally the rejection of “active” galaxies. We use a fixed gap of 1250 km s^{-1} which seemed appropriate when a small number of galaxies is considered (cf. § 3.1). Only a fraction ($\sim 20\%$) of the simulated clusters survive to the procedure of the rejection of interlopers. These clusters contain typically 5–6 members to compute the velocity dispersion, $\sigma_{v,i}$, and the associate statistical error, $\Delta\sigma_{v,i}$. For each of the 20 clusters we compute the median value, $\langle \sigma_{v,i} \rangle_{ran}$, and the s.d., $\sigma_{ran}(\sigma_{v,i})$, of the velocity dispersions of the corresponding simulated clusters, as well as the median statistical error $\langle \Delta\sigma_{v,i} \rangle_{ran}$.

We verify the robustness of our estimates of velocity dispersions by computing the median value and 90% c.l. errors of $\sigma_v / \langle \sigma_v \rangle_{ran}$ within the sample of 20 clusters: we obtain $\langle (\sigma_v / \langle \sigma_v \rangle_{ran}) \rangle_{20} = 1.01_{-0.09}^{+0.08}$ (fixed gaps of 1000 or 1500 km s^{-1} give values of $\langle (\sigma_v / \langle \sigma_v \rangle_{ran}) \rangle_{20} = 1.10$ or 0.97, again consistent with unity).

These simulations also allow us to estimate the global error on the estimate of the velocity dispersion, i.e. the error associated to the procedure of member selection in addition to the statistical error connected to the selected members. On the whole sample of 20 clusters, the median value of the s.d. of velocity dispersions of simulated clusters is very high, $\langle \sigma_{ran}(\sigma_{v,i}) \rangle_{20} \sim 850 \text{ km s}^{-1}$, much larger than the corresponding statistical error, $\langle (\langle \Delta\sigma_{v,i} \rangle_{ran}) \rangle_{20} \sim 350 \text{ km s}^{-1}$. Therefore, in the case of a very small number of available redshifts, the error associated to the

member selection procedure can be more important than the statistical one. However, this kind of error rapidly decreases as the amount of available data increases. For instance, we obtain a global error of $\sim 500 \text{ km s}^{-1}$ vs. a statistical error of 300 km s^{-1} for simulated clusters of 15 galaxies (on average 6–7 members) and the two error estimates become comparable for those clusters containing at least ten members.

As for the poor spatial extension, as suggested by the VDPs of Figure 1, the effect of individual clusters may be large. To be more quantitative, we consider the 11 clusters sampled out to R_{vir} and the corresponding velocity dispersions within $R_{\text{vir}}/2$: the estimate of velocity dispersion varies by $\sim 25\%$ for three clusters. When considering the velocity dispersions within $R_{\text{vir}}/4$ the variation is more than 25% for six clusters and reaches 65% for one cluster. Unfortunately, since the shape of VDPs range different behaviors, the effect cannot be predicted for individual clusters, although strongly decreasing/increasing profiles in the external sampled regions suggest that more correct estimates of velocity dispersions would need data over larger field of view (cf., e.g. AS506, CL0017-20, CL0054-27, and 3C295).

Another effect concerns the sampling within non circular apertures. Since in our sample the elongation of the sampled region is not extreme ($R_{\text{max},c}/R_{\text{max}} \sim 0.6$), we expect that this effect is smaller than the previous one. One can quantify the effect by increasing the weight for external cluster regions in the standard estimate of velocity dispersion $\sigma_{\text{vie}}^2 = [\sigma_{\text{vi}}^2(N_i - 1) + \sigma_{\text{ve}}^2(N_e - 1)] / (N_i + N_e - 1)$, where σ_{vi} and σ_{ve} are the velocity dispersions as computed on the internal and external cluster regions containing N_i and N_e galaxies, respectively. Possible undersampling in the external regions can be corrected for by artificially increasing N_e . We compute σ_{vi} and σ_{ve} inside and outside $R_{\text{max},c}$ for the 35 clusters with at least 10 galaxies: a reasonable increase of the weight (by a factor four) for the external region leads to variations for individual clusters of the order of $\lesssim 7\%$.

Finally, we check the effect of changing the classification of “active” galaxies. We consider the 22 clusters where authors classified also galaxies with ongoing moderate star formation, possibly spiral-like galaxies: for the data by Dressler et al. (1999) we consider “e(c)” galaxies (with moderate absorption plus emission, spiral-like); for the CNOC clusters we consider galaxies classified with “4” (Sbc), and for the clusters by Couch and collaborators we consider “Sp” galaxies (spiral-like, with spectra and color properties of normal nearby spiral galaxies). For these 22 clusters we compare the velocity dispersions as computed in § 4.1, σ_v , with those computed rejecting also spiral-like galaxies as defined above, σ_{v-S} . This different definition of “active” galaxies does not affect the estimate of velocity dispersions. We find no difference between the cumulative distributions of σ_v and σ_{v-S} (using both the Kolmogorov–Smirnov and the Wilcoxon tests, e.g. Press et al. 1992), the median value of σ_v/σ_{v-S} being consistent with unity. Moreover, as for individual clusters, σ_v and σ_{v-S} never

differ by more than 10%.

5 “ACTIVE” AND NON “ACTIVE” GALAXIES

There is evidence that the spatial distribution and kinematics of late-type galaxies (or blue galaxies or ELGs) are different from those of early-type galaxies (or red galaxies or NELGs); these differences lead to higher estimates of internal velocity dispersion and mass for clusters (e.g., Moss & Dickens 1977; Biviano et al. 1997; Mohr et al. 1996; Carlberg et al. 1997a; Koranyi & Geller 2000). Biviano et al. (1997) suggested that the dynamical state of the ELGs, which are often spirals of late types or irregulars, reflects the phase of galaxy infall rather than the virialized condition in the relaxed cluster core. Carlberg et al. (1997a) suggested that, although differing in their distributions, both blue and red galaxies are in dynamical equilibrium with clusters.

We check if the populations of “active” and non “active” galaxies, AGs and NAGs, really differ in their kinematics. Since we often classify AGs on the base of the presence of emission lines in their spectra (but see Couch et al. 1998 for the use of colors, too) this classification roughly corresponds to the one between ELGs and NELGs.

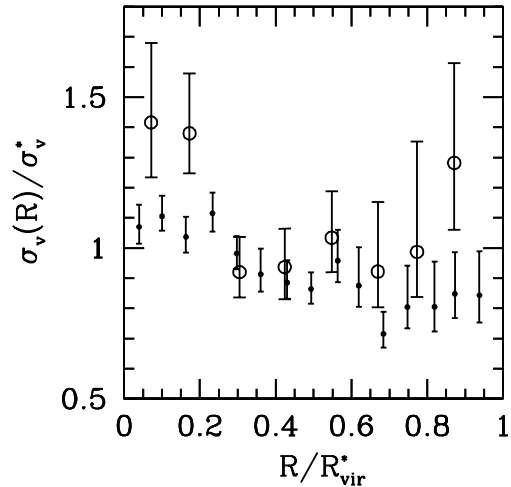


Fig. 3.— The (normalized) line-of-sight velocity dispersion, $\sigma_v(R)$, as a function of the (normalized) projected distance from the cluster center. The points represent data combined from all clusters and binned in equispacial intervals. Open and filled circles are obtained using the “active” galaxies, AGs, and the galaxies without strong signs of activity, NAGs, respectively. The normalizing quantities are computed combining both the AGs and NAGs. We give the robust estimates of velocity dispersion and the respective bootstrap errors.

We consider the 43 out of 51 clusters for which spectral information is available, each cluster containing $N_{\text{NAG}} (= N_m)$ NAGs and $N_{\text{AG}} (= N_g - N_m)$ AGs, cf. Table 2. Figure 3 shows that the σ_v profile of the AGs is generally higher than the profile of the NAGs, where the profiles

are obtained combining together galaxies of all 43 clusters and normalizing to the values of σ_v and R_{vir} obtained for clusters before the rejection of the AGs (otherwise the difference would be also larger). A two-dimensional Kolmogorov–Smirnov test (Fasano & Franceschini 1987) applied to the normalized velocities and distances found a difference larger than $> 99\%$ between the two galaxy populations.

Only for 19 of the 43 clusters there are enough galaxies ($N_{AG} \geq 5$ and $N_{NAG} \geq 5$) to compute and compare the respective AG and NAG σ_v . Figure 4 shows the comparison between cumulative distributions of σ_v , as computed considering the AGs or NAGs. The AG σ_v -distribution shows a tail at high σ_v , which, however, is not significant according to a Kolmogorov–Smirnov test, and only slightly significant at the 93% c.l. according to the Wilcoxon test (e.g., Press et al. 1992). To test for different means and dispersions of the AG and NAG populations in each individual cluster, we apply the standard means-test and F-test (e.g., Press et al. 1992). We find evidence of a difference more significant than $> 95\%$ only for A851 ($\sigma_{AG} = 1761 \text{ km s}^{-1} \neq \sigma_{NAG} = 1067 \text{ km s}^{-1}$ at the $\sim 98\%$ c.l.) and for CL1602+4304 ($\langle V \rangle_{AG} = 268653 \text{ km s}^{-1} \neq \langle V \rangle_{NAG} = 270349 \text{ km s}^{-1}$ at the $\sim 96\%$ c.l.).

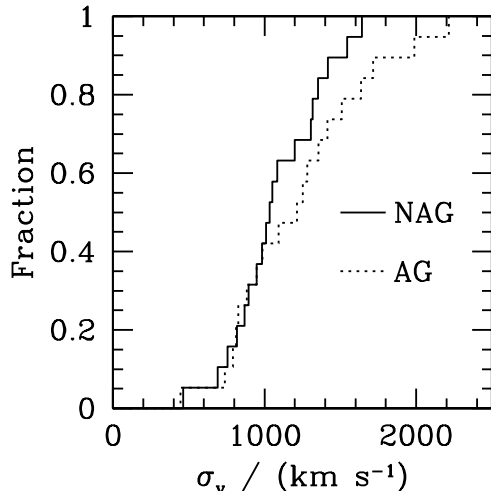


Fig. 4.— The cumulative distributions of line-of-sight velocity dispersion computed using the “active” galaxies, AGs, and the galaxies without strong signs of activity, NAGs, as indicated by dotted and solid lines, respectively.

The evidence of difference between the two populations is in agreement with previous findings for nearby and distant clusters (e.g., Biviano et al. 1997; Dressler et al. 1999; Mohr et al. 1996). A really quantitative comparison of the effect is complicated by the differences in the definition of “active” galaxies. By using ENACS clusters, Biviano et al. (1997) found that σ_v of ELGs is, on average, 20% larger than that of NELGs, and we find $\langle \sigma_{AG}/\sigma_{NAG} \rangle = 1.12 \pm 0.07$. As for the combined velocity dispersion profile (cf. Figure 3), our result in central

cluster regions ($R \lesssim 0.1 h^{-1} \text{ Mpc}$) is similar to that of Biviano et al (1997) giving higher central σ_v for AGs (and ELGs) than for NAGs (and NELGs), i.e. $\sim 1.4 \pm 0.2$ vs. $\sim 1.1 \pm 0.05$ for normalized σ_v . Our last point of the velocity dispersion profile is instead very high, but we suspect that it could be due to the loss of efficiency in rejecting interlopers in very poorly sampled external regions of distant clusters.

6 COMPARISON WITH RESULTS FROM X-RAY AND LENSING DATA

We collect X-ray luminosities, in general bolometric ones, $L_{bol,X}$, and temperature, T_X , for 38 and 22 clusters, respectively. For A223, A521, CL0054-27, CL0412-65, CL1604+4304, and the four clusters by Bower et al. (1997) we obtain the bolometric luminosities by multiplying the original band luminosities by a temperature-dependent bolometric correction factor. This factor is computed under the assumptions of pure bremsstrahlung intracluster medium emission and a power-law approximation for the Gaunt factor. For the correction we use the temperatures estimated from σ_v in the hypothesis of density energy equipartition between hot gas and galaxies, i.e. $\beta_{spec} = \sigma_v^2/(kT/\mu m_p) = 1$, where $\mu = 0.58$ is the mean molecular weight and m_p the proton mass. For the four clusters by Bower et al. (1997), which have very few galaxies with measured redshift, we use the $L_X - \sigma_v$ relation given by the authors for nearby clusters. For these four clusters we expect $\sigma_v \sim 600 \text{ km s}^{-1}$, i.e. $T \sim 2 \text{ keV}$.

In Table 4 we list the collected values for $L_{bol,X}$, and T_X with the corresponding reference sources (Cols. 2–5), and the value of β_{spec} (Col. 6). The errors on β_{spec} take into account errors on both σ_v and T_X .

Figure 5 shows the $L_{X,bol} - \sigma_v$ relation compared to that found by Borgani et al. (1999) for nearby clusters. Excluding the leftmost point (J2175.15TR), the resulting bisecting linear regression is

$$\log(L_{bol,X}/10^{44} \text{ erg s}^{-1}) = 4.4^{+1.8}_{-1.0} \log(\sigma_v/\text{km s}^{-1}) - 12.6^{+3.0}_{-5.4}, \quad (6)$$

where errors come from the difference with respect to the direct and the inverse linear regression (Isobe et al. 1990, OLS methods). Our $L_{bol,X} - \sigma_v$ relation is consistent with that of nearby clusters (e.g., White et al. 1997; Borgani et al. 1999; Wu, Xue, & Fang 1999). As for the point excluded, note that our analysis of J2175.15TR is based only on 19 galaxies, and the estimate of σ_v is recovered from only eight member galaxies (with an error larger than 100%).

All clusters for which σ_v should be better interpreted as an upper limit to the true estimate (AS506, CL0054-27, 3C295) lie on the right-upper corner of the plot. Excluding these points we fit a consistent relation, i.e. $\log(L_{bol,X}/10^{44} \text{ erg s}^{-1}) = 4.7^{+1.9}_{-1.1} \log(\sigma_v/\text{km s}^{-1}) - 13.5^{+3.1}_{-5.5}$.

Figure 6 shows the $\sigma_v - T_X$ relation compared to that of nearby clusters, as reported by G98. As for distant

TABLE 4
COMPARISON WITH X-RAY PROPERTIES

Cluster Name	$L_{X,bol}$ $h^{-2} 10^{44} \text{ erg s}^{-1}$	References	T_X keV	References	β_{spec}
(1)	(2)	(3)	(4)	(5)	(6)
A115S	2.26375	1	-	-	-
A222	1.9125	2	-	-	-
A223 ^a	0.7	3	-	-	-
A370 ^b	5.1925	2	$7.13^{+1.05}_{-0.83}$	2	$0.63^{+0.18}_{-0.17}$
A520 ^b	9.3375	2	$8.59^{+0.93}_{-0.93}$	2	$0.71^{+0.33}_{-0.19}$
A521 ^a	2.72	4	-	-	-
A665 ^b	10.43	2	$8.26^{+0.95}_{-0.81}$	2	$0.49^{+0.28}_{-0.16}$
A851 ^b	4.02	2	$6.7^{+2.7}_{-1.7}$	2	$1.03^{+0.31}_{-0.25}$
A1300 ^b	11.9075	2	$11.4^{+1.3}_{-1.0}$	11	$0.57^{+0.11}_{-0.12}$
A2218 ^b	5.49	2	$7.05^{+0.36}_{-0.35}$	2	$1.28^{+0.31}_{-0.23}$
A2390 ^b	15.8725	2	$11.1^{+1.5}_{-1.6}$	2	$0.91^{+0.13}_{-0.13}$
A3888	7.85	2	-	-	-
AS506 ^b	4.3775	2	$7.2^{+3.7}_{-1.8}$	2	$1.55^{+0.68}_{-0.42}$
AS1077 ^b	9.525	2	$9.76^{+1.04}_{-0.85}$	2	$1.20^{+0.23}_{-0.14}$
CL0024+16 ^b	1.5225	5	$5.7^{+4.9}_{-2.1}$	5	$0.88^{+0.50}_{-0.29}$
CL0054-27 ^a	0.4325	6	-	-	-
CL0303+17	0.9	7	-	-	-
CL0412-65 ^a	0.1325	6	-	-	-
CL1447+26	2.6725	2	-	-	-
CLJ1604+4304 ^a	0.535	8	-	-	-
1E0657-56 ^b	30.	9	$11.7^{+2.2}_{-1.4}$	12	$0.44^{+0.18}_{-0.11}$
F1637.23TL ^a	0.2725	10	-	-	-
F1652.20CR ^a	0.2225	10	-	-	-
J2175.15TR ^a	0.3625	10	-	-	-
J2175.23C ^a	0.0875	10	-	-	-
MS0015.9+1609 ^b	7.0325	2	$8.0^{+1.0}_{-1.0}$	2	$0.73^{+0.20}_{-0.15}$
MS0302.7+1658	2.27	2	$4.6^{+0.8}_{-0.8}$	2	$0.71^{+0.24}_{-0.20}$
MS0302.5+1717	1.0575	2	-	-	-
MS0440.5+0204 ^b	1.857	2	$5.30^{+1.27}_{-0.85}$	2	$0.80^{+0.28}_{-0.28}$
MS0451.6-0305	3.9825	2	$10.17^{+1.55}_{-1.26}$	2	$1.03^{+0.22}_{-0.18}$
MS1008.1-1224 ^b	2.2825	2	$7.29^{+2.45}_{-1.52}$	2	$0.89^{+0.27}_{-0.21}$
MS1054.4-0321 ^b	4.9775	2	$12.3^{+3.1}_{-2.2}$	2	$0.68^{+0.19}_{-0.15}$
MS1224.7+2007	2.015	2	$4.3^{+0.7}_{-0.6}$	2	$0.99^{+0.29}_{-0.24}$
MS1358.4+6245 ^b	5.4525	2	$7.5^{+7.1}_{-1.5}$	2	$0.78^{+0.47}_{-0.14}$
MS1512.4+3647 ^b	1.905	2	$3.57^{+1.33}_{-0.64}$	2	$1.02^{+0.51}_{-0.29}$
MS1621.5+2640	2.055	2	-	-	-
RXJ1716+67	4.35	2	$5.66^{+1.37}_{-0.58}$	2	$2.24^{+1.04}_{-0.71}$
3C295 ^b	6.5	2	$7.13^{+2.06}_{-1.35}$	2	$2.29^{+0.75}_{-0.59}$

^a Bolometric luminosity here computed from the original band luminosity.

^a Errors on T_X are at the 90% c.l.; they are rescaled by a factor 1.6 to compute 68% c.l. errors on β_{spec} .

(1) White et al. 1997; (2) Wu et al. 1999 (see this compilation for original data sources); (3) Lea & Henry 1988; (4) Ulmer et al. 1985; (5) Soucail et al. 2000; (6) Smail et al. 1997; (7) Kaiser et al. 1998; (8) Castander et al. 1994; (9) Tucker et al. 1998; (10) Bower et al. 1997; (11) Pierre et al. (1999); (12) Yaqoob 1999.

clusters, the data have a too small dynamical range to attempt a linear fit: the visual inspection of Figure 6 suggests no difference with nearby clusters in agreement with the result of by Mushotzky & Scharf (1997) and Wu et al. (1999). We obtain $\beta_{spec} = 0.88^{+0.14}_{-0.17}$ (median value with errors at the 90% c.l.), in agreement with the value of $\beta_{spec} = 0.88 \pm 0.04$ for nearby clusters (cf. G98). Moreover, we find no correlation between β_{spec} and redshift (cf. also Wu et al. 1999).

Under the assumption that the hot diffuse gas is in hy-

drostatic and isothermal equilibrium with the underlying gravitational potentials of clusters, one can obtain the X-ray cluster masses provided that the gas temperature and radial profile of gas distribution are known (e.g. Wu et al. 1998). The availability of T_X allow us to compute the mass within R_{vir} for 22 clusters according to $M_X = (3\beta_{fit,gas}kT \cdot R_{vir}) / (G\mu m_p) \cdot (R_{vir}/R_x)^2 / [1 + (R_{vir}/R_x)^2]$, where we adopt the gas distribution given by the β -model with typical parameters (slope $\beta_{fit,gas} = 2/3$ and core radius $R_x = 0.125 h^{-1} Mpc$, e.g. Jones & Forman 1992).

We find mass values consistent with our optical virial estimates, i.e. $M/M_X = 1.02$ (0.86–1.32) for the median value and the range at the 90% c.l..

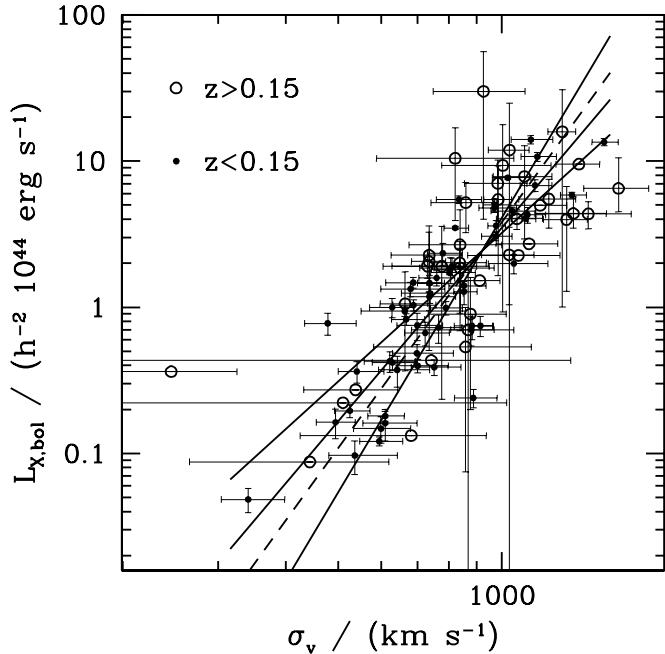


Fig. 5.— $L_{X,bol}$ - σ_v relation for distant (open circles) and nearby clusters (filled circles). For the nearby clusters we show results as reported by Borgani et al. (1999), all having σ_v estimated at least with 30 galaxy redshifts (Girardi et al. 1998b) and also belonging to the X-ray Brightest Abell-like Cluster survey (Ebeling et al. 1996). The error bands at the 68% c.l. are shown: errors on $L_{X,bol}$ are not available for a few distant clusters. The three solid lines are direct, inverse, and bisecting linear regression for the distant clusters (obtained rejecting the point on the left). The dashed line is the bisecting linear regression for the nearby clusters as computed by Borgani et al. (1999).

As for gravitational lensing masses, we resort to estimates found in the literature. We collect projected estimates from weak gravitational lensing analysis, M_L , for 18 clusters. In order to compare our optical virial masses to M_L , we project and rescale our masses M within the corresponding radius using the fitted galaxy spatial distribution. In Table 5 we list the reference sources (Col. 2) from where we take R_L and M_L (Cols. 3 and 4); the corresponding optical virial projected mass, $M_{opt,L}$ (Col. 5); and the respective ratio (Col. 6). We obtain $M_{opt,L}/M_L = 1.30$ (0.63–2.13) (median value and range at the 90% c.l.). Moreover, we do not find any correlation between M/M_X or $M_{opt,L}/M_L$ and redshift.

Our findings are in agreement with other recent studies which find, on average, no evidence of discrepancy between different mass estimates as computed within large radii, thus suggesting that distant clusters are not far from global dynamical equilibrium (e.g., Allen 1998; Wu et al. 1998; Lewis et al. 1999). Note that we avoid to consider

mass determination in very central cluster regions since our analysis of cluster members give poor constraints on mass distribution on these scales. Indeed, the assumption of dynamical equilibrium seem to break down in the very central regions as suggested by comparisons with strong lensing mass estimates (e.g., Allen 1998; Lewis et al. 1999; Wu et al. 1998).

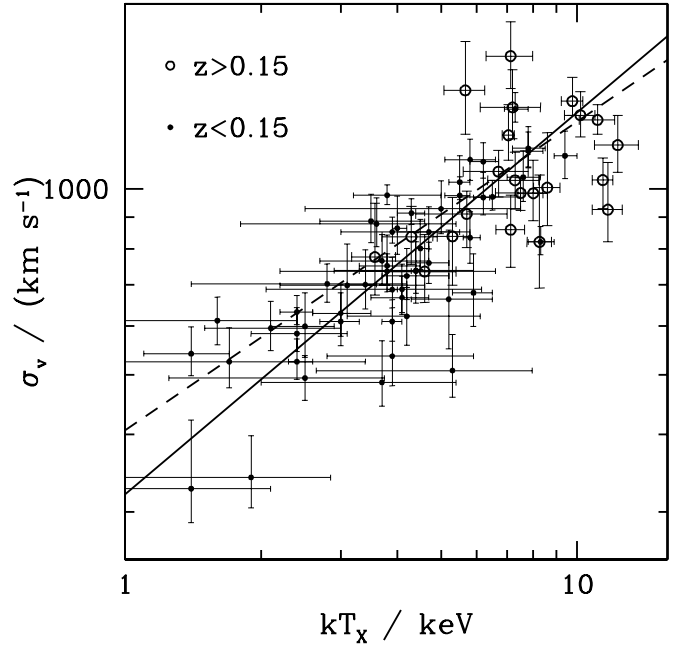


Fig. 6.— σ_v - T_X relation for distant (open circles) and nearby clusters (filled circles). For the nearby clusters we show results as reported by Girardi et al. (1998b), all having σ_v estimated at least with 30 galaxy redshifts, and T_X taken from David et al. (1993) and from White et al. (1997). The error bands at the 68% c.l. are shown: when authors give only 90% c.l. errors on T_X , we apply a reduction by a factor of 1.6. The solid line is the bisecting linear regression for the nearby clusters as computed by Girardi et al. (1998b). The dashed line represents the model with the equipartition of energy per unit mass between gas and galaxy components ($\beta_{spec} = 1$).

7 SUMMARY AND CONCLUSIONS

In order to properly analyze the possible dynamical evolution of galaxy clusters we apply the same procedures already applied on a sample of nearby clusters (170 clusters at $z < 0.15$ from ENACS and other literature, Girardi et al. 1998b, cf. also Fadda et al. 1996) to a corresponding sample of 51 distant clusters ($0.15 \lesssim z \lesssim 0.9$, $\langle z \rangle \sim 0.3$). Each cluster has at least 10 galaxies with available redshift in the literature. Three cluster fields show two overlapping peaks in their velocity distribution and large uncertainties in their dynamics. Out of other cluster fields, 45 fields show only one peak in the velocity distribution and three fields show two separable peaks, for a total of 51 well-defined cluster systems. These 51 systems are those

TABLE 5
COMPARISON WITH MASSES FROM WEAK GRAVITATIONAL LENSING

Name	References	R_L $h^{-1} Mpc$	M_L $h^{-1} 10^{14} M_\odot$	$M_{opt,L}$ $h^{-1} 10^{14} M_\odot$	$M_{opt,L}/M_L$
(1)	(2)	(3)	(4)	(5)	(6)
A851	1	0.375	$3.0^{+0.5}_{-0.5}$	$3.792^{+1.140}_{-1.168}$	$1.26^{+0.43}_{-0.44}$
A2218	2	0.4	$3.9^{+0.7}_{-0.7}$	$5.206^{+1.806}_{-1.599}$	$1.33^{+0.52}_{-0.47}$
A2390	3	0.59	$10.0^{+3.5}_{-3.6}$	$5.697^{+1.574}_{-1.542}$	$0.57^{+0.25}_{-0.25}$
AS1077	4	0.25	$2.0^{+0.2}_{-0.2}$	$4.424^{+1.374}_{-1.195}$	$2.21^{+0.72}_{-0.64}$
CL0024+16	5	0.2	$1.38^{+0.37}_{-0.37}$	$0.979^{+0.300}_{-0.336}$	$0.71^{+0.29}_{-0.31}$
CL0054-27	5	0.2	$1.71^{+0.64}_{-0.64}$	$0.593^{+0.969}_{-0.278}$	$0.35^{+0.58}_{-0.21}$
CL0303+17	6	0.592	$0.981^{+0.312}_{-0.312}$	$3.307^{+1.366}_{-1.342}$	$3.37^{+1.76}_{-1.74}$
CL0412-65	5	0.2	$0.25^{+0.41}_{-0.41}$	$0.749^{+0.593}_{-0.448}$	$3.00^{+5.46}_{-5.23}$
CL1601+42	5	0.2	$0.77^{+0.66}_{-0.66}$	$0.729^{+0.263}_{-0.268}$	$0.95^{+0.88}_{-0.88}$
MS0015.9+1609	5	0.2	$1.87^{+0.64}_{-0.64}$	$1.120^{+0.408}_{-0.354}$	$0.60^{+0.30}_{-0.28}$
MS0302.7+1658	6	0.596	$0.624^{+0.315}_{-0.315}$	$1.539^{+0.597}_{-0.510}$	$2.47^{+1.57}_{-1.49}$
MS0302.5+1717	6	0.595	$2.069^{+0.387}_{-0.387}$	$1.998^{+0.642}_{-0.681}$	$0.97^{+0.36}_{-0.38}$
MS1008.1-1224	7	0.34	$2.18^{+0.47}_{-0.47}$	$3.308^{+1.108}_{-1.066}$	$1.52^{+0.60}_{-0.59}$
MS1054.4-0321	8	0.8	$8^{+21.}_{-5.}$	$5.049^{+1.736}_{-1.591}$	$0.63^{+1.67}_{-0.83}$
MS1224.7+2007	9	0.65	$4.7^{+2.0}_{-1.5}$	$2.258^{+0.781}_{-0.721}$	$0.48^{+0.26}_{-0.23}$
MS1358.4+6245	10	0.5	$2.2^{+0.3}_{-0.3}$	$3.791^{+1.048}_{-1.061}$	$1.72^{+0.53}_{-0.54}$
RXJ1716+67	11	0.5	$2.6^{+0.9}_{-0.9}$	$5.607^{+2.638}_{-2.197}$	$2.16^{+1.26}_{-1.13}$
3C295	5	0.2	$2.35^{+0.38}_{-0.38}$	$5.014^{+1.855}_{-1.696}$	$2.13^{+0.86}_{-0.80}$

(1) Seitz et al. 1996; (2) Squires et al. 1996a; (3) Squires et al. 1996b; (4) Natarajan et al. 1998; (5) Smail et al. 1997; (6) Kaiser et al. 1998; (7) Athreya et al. 1999, see also Lombardi et al. 2000; (8) Luppino & Kaiser 1997; (9) Fischer 1999; (10) Hoekstra et al. 1998; (11) Clowe et al. 1998.

used in the comparison with nearby clusters (i.e., 160 well-defined systems, cf. § 3 of Girardi et al. 1998b).

We select member galaxies, analyze the velocity dispersion profiles, and evaluate in a homogeneous way cluster velocity dispersions and virial masses.

As a main general result, we do not find any significant evidence for dynamical evolution of galaxy clusters. More in detail, our results can be summarized as follows.

- The galaxy spatial distribution is similar to that of nearby clusters, i.e. the fit to a King-like profile gives a two-dimensional slope of $\alpha = 0.7$ and a very small core radius of $R_c = 0.05 h^{-1} Mpc$. Note that we do not want to really asses the existence of a core, or to state that the King-modified profile is better than other forms for galaxy density profiles; the King-modified profile is used for a consistent comparison with nearby clusters. We refer to Girardi et al. (1998b, § 8) for other relevant analyses and discussions.
- For those clusters with good enough data, the integrated velocity dispersion profiles show a behavior similar to those of nearby clusters: they are strongly increasing or decreasing in the central cluster regions, but always flattening out in the external regions, thus suggesting that large-scale dynamics is not affected by velocity anisotropies.
- The average velocity dispersion profile can be explained by a model with isotropic orbits, which well describe also nearby clusters. Possible evidences for more radial orbits are not statistically significant.

- There is no evidence of evolution in both $L_{bol,X-\sigma_v}$ and σ_v-T_X relations, thus in agreement with previous results (Mushotzky & Scharf 1997; Borgani et al. 1999).

Moreover, within the large scatter of present data, we find, on average, no significant evidence of discrepancies between our virial mass estimates and those from X-ray and gravitational lensing data, thus suggesting that distant clusters are not far from global dynamical equilibrium (cf. also Allen 1998; Lewis et al. 1999; Wu et al. 1998).

We conclude that the typical redshift of cluster formation is higher than that of our sample in agreement with previous suggestions (e.g., Schindler 1999; Mushotzky 2000). In particular, we agree with preliminary results by Adami et al. (1999), who applied the same techniques used for the nearby ENACS clusters on 15 distant clusters, ($< z > \sim 0.4$) from the Palomar Distant Cluster Survey (Postman et al. 1996).

Although some clusters at very high redshift, e.g. $z > 0.8$, are already known (e.g., Gioia et al. 1999; Rosati et al. 1999), the construction of a large cluster sample useful for studying internal dynamics will require a strong observational effort. Note that, already in the construction of the cluster sample analyzed here, we relax the requirements applied to the sample of nearby clusters by Girardi et al. (1998b), i.e. the distant clusters are more poorly sampled. Throughout the presentation of our analyses we stress how both the poor number of galaxies and the small spatial extension of some clusters can affect the robustness

of their resulting properties. In particular, Monte Carlo simulations, which take into account the whole membership procedure, show that the estimate of velocity dispersion is, on average, well recovered also in the case of very poor sampling (only 10 galaxies in the cluster field giving 5–6 members), but that the global error associated to the individual clusters should be a factor ~ 2.5 larger than the pure statistical error. Also the small spatial extension could lead to large over/underestimates of velocity dispersion of individual clusters: we evaluate that variations of 25% are quite common when clusters are sampled only out to half of the virialization region.

We thank the anonymous referee for useful suggestions and comments. We also thank Andrea Biviano and Stefano Borgani for interesting discussions, and Massimo Ramella for providing us redshifts and positions of galaxies for 1E0657-56. Special thanks to Alenka Devetak for her help in initial phase of this project. This research has made use of the NASA/IPAC Extragalactic Database (NED) which is operated by the Jet Propulsion Laboratory, California Institute of Technology, under contract with the National Aeronautics and Space Administration. This work has been partially supported by the Italian Ministry of University, Scientific Technological Research (MURST), by the Italian Space Agency (ASI), and by the Italian Research Council (CNR-GNA).

APPENDIX A RESULTS FOR MULTIPEAKED CLUSTERS

Here we shortly present the results of our analysis for the three clusters with uncertain dynamics, i.e. with two peaks in the velocity distribution which are not clearly separable. We consider both the system composed by the two peaks together and each peak individually. In Figure 7 we plot the velocity-space galaxy density for each cluster, as pro-

vided by the adaptive-kernel reconstruction method, and the integrated velocity dispersion profile VDP for each possible system. Table 6 summarizes the results of the analysis of the internal dynamics. Note the strong variation in σ_v and mass when considering the two peaks together or not. Some comments on individual clusters follow.

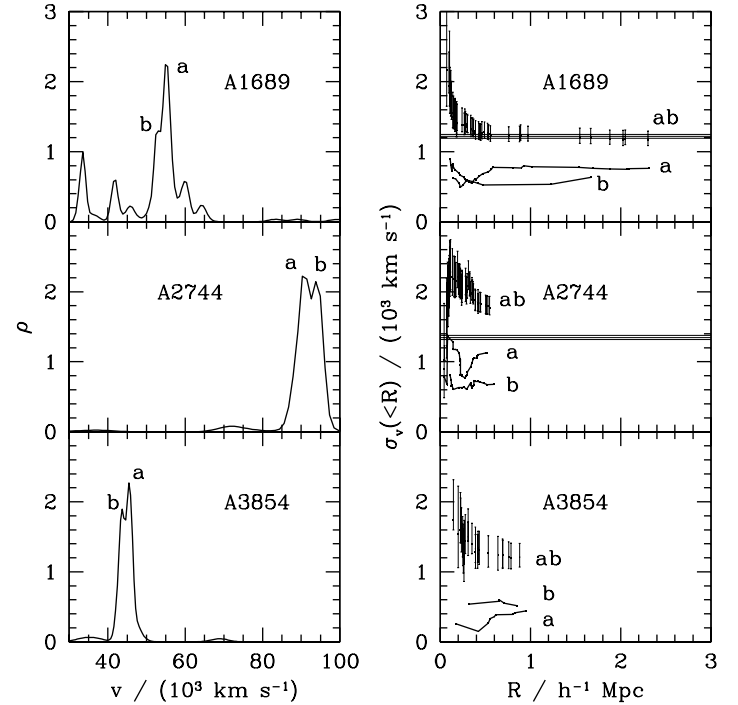


Fig. 7.— For each of the three clusters we give the relative velocity-space galaxy density, as provided by the adaptive kernel reconstruction method (left panels) and integrated line-of-sight velocity dispersion profiles $\sigma_v(<R)$ for each of the considered systems (right panels). For the velocity dispersion profiles we plot bootstrap errors only in the case of the system with joined peaks. The horizontal lines in the right panels represent X-ray temperature with the respective errors taken from Wu et al. (1999) and transformed in σ_v imposing $\beta_{spec} = 1$.

TABLE 6
CLUSTERS WITH UNCERTAIN DYNAMICS

Name	N_m	R_{max}	σ_v	R_{vir}	R_{PV}	T	M_V	M
(1)	(2)	$h^{-1} Mpc$	$km s^{-1}$	$h^{-1} Mpc$	(6)	(7)	$h^{-1} 10^{14} M_\odot$	(9)
A1689a	38	2.26	765^{+80}_{-60}	1.01	0.75	C	$4.81^{+1.57}_{-1.42}$	$4.14^{+1.35}_{-1.22}$
A1689b	15	1.67	636^{+167}_{-127}	0.85	0.65	B	$2.87^{+1.67}_{-1.35}$	$2.27^{+1.32}_{-1.07}$
A1689ab	49	2.26	1172^{+123}_{-99}	1.55	1.07	B	$16.12^{+5.26}_{-4.86}$	$13.02^{+4.25}_{-3.93}$
A2744a	34	0.53	1121^{+176}_{-88}	1.28	0.91	C	$12.59^{+5.05}_{-3.72}$	$10.90^{+4.37}_{-3.22}$
A2744b	25	0.64	682^{+97}_{-75}	0.77	0.60	C	$3.04^{+1.15}_{-1.01}$	$2.60^{+0.98}_{-0.87}$
A2744ab	55	0.59	1777^{+151}_{-125}	2.02	1.34	B	$46.36^{+14.01}_{-13.30}$	$37.66^{+11.38}_{-10.80}$
A3854a	18	0.70	455^{+43}_{-102}	0.63	0.50	-	$1.14^{+0.36}_{-0.59}$	$0.89^{+0.28}_{-0.46}$
A3854b	9	0.75	520^{+163}_{-254}	0.72	0.57	-	$1.68^{+1.13}_{-1.69}$	$1.32^{+0.89}_{-1.33}$
A3854ab	30	0.81	1211^{+210}_{-138}	1.67	1.14	A	$18.31^{+7.83}_{-6.19}$	$10.63^{+4.55}_{-3.60}$

A1689 Teague, Carter, & Gray (1990) computed a value of $\sigma_v = 1989 km s^{-1}$. As for the analysis of the cluster

members, the two peaks in the velocity distribution were already pointed out by Girardi et al. (1996; 1997b) us-

ing the same adaptive kernel method. By using a multi-scale analysis which couples kinematical estimators with the wavelet transform, Girardi et al. (1997b) found the presence of two dynamically relevant structures, but with a smaller σ_v and mass with respect to the two systems, “a” and “b”, analyzed here. Moreover, A1689 is well known for a strong discrepancy between mass from X-ray and strong gravitational lensing analyses (e.g. Miralda-Escudé & Babul 1995) which could be due to its complex structure. Also the very recent weak lensing analysis of Taylor et al. (1998) suggests the model of a double cluster aligned along the line of sight in order to explain discrepancies between optical and X-ray results. These results and the

fact that A1689 appears well aligned along the line of sight with other structures (three foreground groups, Teague et al. 1990) suggests the presence of a large structure filament well aligned along the line of sight.

A2744 Couch & Sharples (1987) computed a value of $\sigma_v = 1947^{+292}_{-201} \text{ km s}^{-1}$. A strong suggestion for the dynamical activity comes from the recent study by Allen (1998): among the 13 clusters analyzed, A2744 shows the strongest discrepancy between mass from X-ray and gravitational lensing analyses.

A3854 Colless & Hewett (1987) listed a value of $\sigma_v = 1180^{+202}_{-143} \text{ km s}^{-1}$.

REFERENCES

- Abell, G.O., Corwin, H. G. Jr., & Olowin, R. P. 1989, *ApJS*, 70, 1
- Abraham, R., Yee, H. K. C., Ellingson, E., Carlberg, R. G., & Gravel, P. 1998, *ApJS*, 116, 231
- Adami, C., Biviano, A., & Mazure, A. 1998, *A&A*, 331, 439
- Adami, C., Holden, B., Mazure, A., Castander, F., Nichol, R., Ulmer, Postman, M., & Lubin, L. 1999, *proc. of the 1999 IGRAP conference*, preprint astro-ph/9907366
- Adami, C., Mazure, A., Katgert, P., & Biviano, A. 1998, *A&A*, 336, 63
- Allen, S. W. 1998, *MNRAS*, 296, 392
- Allen, S. W. Fabian, A. C., Kneib, J. P. 1996, *MNRAS*, 283, 263
- Athreya, R., Mellier, Y., Van Waerbeke, L., Fort (IAP), B., Pello, R., & Dantel-Fort, M. 1999, submitted to *A&A*, preprint astro-ph/9909518
- Bennett, A. S., 1962, *Mem. R. Astron. Soc.*, 68, 163
- Beers, T. C., Flynn, K., & Gebhardt, K. 1990, *AJ*, 100, 32
- Beers, T. C., Geller, M. J., & Huchra, J. P. 1983, *ApJ*, 264, 356
- Bird, C. M., Mushotzky, R. F., & Metzler, C. A. 1995, *ApJ*, 453, 40
- Biviano, A., Katgert, P., Mazure, A., Moles, M., den Hartog, R., Perea, J., & Focardi, P. 1997, *A&A*, 321, 84
- Borgani, S., Girardi, M., Carlberg, R. G., Yee, H. K. C., & Ellingson, E. 1999, *ApJ*, 527, 561
- Borgani, S., Rosati, P. R., Della Ceca, R., Tozzi, P., & Norman, C. 2000, *astro-ph/9912378*
- Bower, R. G., Castander, F. J., Couch, W. J., Ellis, R. S., & Böhringer, H. 1997, *MNRAS*, 291, 353
- Burke, D. J., Collins, C. A., Sharples, R. M., Romer, A. K., Holden, B.P., & Nichol, R. C. 1997, *ApJ*, 488, 83
- Butcher, H.R., & Oemler, A.Jr. 1978, *ApJ*, 219, 18
- Cappi, A., Held, E. V., & Marano, B. 1998, *ApJS*, 129, 31
- Carlberg, R. G., et al. 1997a, *ApJ*, 476, L7
- Carlberg, R.G., Morris, S.L., Yee, H.K.C., & Ellingson, E. 1997b, *ApJ*, 479, L19
- Carlberg, R. G., Yee, H. K. C., Ellingson, E., Abraham, R., Gravel, P., Morris, S., & Pritchett, C. J. 1996, *ApJ*, 462, 32
- Carlberg, R. G., Yee, H. K. C., & Ellingson, E. 1997c, *ApJ*, 478, 462
- Castander, F. J., Ellis, R. S., Frenk, C. S., Dressler, A., & Gunn, J. E. 1994, *ApJ*, 424, L79
- Clowe, D., Luppino, G. A., Kaiser, N., Henry, J. P., & Gioia, I. M. 1998, *ApJ*, L61
- Colafrancesco, S., & Vittorio, N. 1994, *ApJ*, 433
- Colless, M., & Hewett, P. 1987, *MNRAS*, 224, 453
- Collins, C. A., Guzzo, L., Nichol, R. C., & Lumsden, S. L. 1995, *MNRAS*, 274, 1071
- Couch, W. J., Barger, A. J., Smail, I., Ellis, R. S., & Sharples, R. M. 1998, *ApJ*, 497, 188
- Couch, W. J., Ellis, R. S., MacLaren, I., & Malin, D. F. 1991, *MNRAS*, 249, 606
- Couch, W. J., Ellis, R. S., Sharples, R. M., & Smail, I. 1994, *ApJ*, 430, 121
- Couch, W. J., Newell, E. B. 1984, *ApJS*, 56, 143
- Couch, W. J., & Sharples, R. M. 1987, *MNRAS*, 229, 423
- Danese, L., De Zotti, C., & di Tullio, G. 1980, *A&A*, 82, 322
- David, L. P., Slyz, A., Jones, C., & Forman, W., Vrtilik, S. D., & Arnaud, K. A. 1993, *ApJ*, 412, 479
- De Grandi, S., et al. 1999, *ApJ*, 514, 148
- den Hartog, R., & Katgert, P. 1996, *MNRAS*, 279, 349
- Donahue, M., & Voit, G. M. 1999, *ApJ*, 523, L137
- Dressler, A., et al. 1997, *ApJ*, 490, 577
- Dressler, A., & Gunn, J. E. 1992, *ApJS*, 78, 1
- Dressler, A., Smail, I., Poggianti, B. M., Butcher, H., Couch, W. J., Ellis, R. S., & Oemler, A. Jr. 1999, *ApJS*, 122, 51
- Ebeling, H., Voges, W., Böhringer, H., Edge, A.C., Huchra, J.P., & Briel, U.G. 1996, *MNRAS*, 281, 799
- Eke, V. R., Cole, S., & Frenk, C. S. 1996, *MNRAS*, 282, 263
- Ellingson, E., Yee, H. K. C., Abraham, R., Morris, S. L., & Carlberg, R. G. 1998, *ApJS*, 116, 247
- Ellingson, E., Yee, H. K. C., Abraham, R., Morris, S. L., Carlberg, R. G., Smeecker-Hane, T. A. 1996, *ApJS*, 113, 1
- Ellingson, E., Yee, H. K. C., Green, R. F., & Kinman, T. D. 1989, *AJ*, 97, 1539
- Fabricant, D. G., Bautz, M. W., & McClintock, J. E. 1994, *AJ*, 107, 8
- Fadda, D., Girardi, M., Giuricin, G., Mardirossian, F., & Mezzetti, M. 1996, *ApJ*, 473, 670 (F96)
- Fan, X., Bahcall, N. A., & Cen, R. 1997, *ApJ*, 490, L123
- Fasano, G., & Franceschini, A. 1987, *MNRAS*, 225, 155
- Fischer, P. 1999, *AJ*, 117, 2024
- Forman, W., Bechtold, J., Blair, W., Giacconi, R., van Speybroeck, L., & Jones, C. 1981, *ApJ*, 243, L133
- Garilli, B., Maccagni, D., & Vettolani, G. 1991, *AJ*, 101, 795
- Gioia, I. M., Henry, J. P., Maccacaro, T., Morris, S. L., Stocke, J. T., & Wolter, A. 1990, *ApJ*, 356, L35
- Gioia, I. M., Henry, J. P., Mullis, C. R., & Ebeling, H. 1999, *AJ*, 117, 2608
- Gioia, I. M., Maccacaro, T., Schild, R. E., Wolter, A., Stocke, J. T., Morris, S. L., & Henry, J. P. 1990, *ApJS*, 72, 567
- Gioia, I. M., Shaya, E. J., Le Fèvre, O., Falco, O. O., Luppino, G. A., & Hammer, F. 1998, *ApJ*, 497, 573
- Girardi, M., Biviano, A., Giuricin, G., Mardirossian, F., & Mezzetti, M. 1995, *ApJ*, 438, 527
- Girardi, M., Borgani, S., Giuricin, G., Mardirossian, F., & Mezzetti, M. 1998a, *ApJ*, 506, 45
- Girardi, M., Escalera, E., Fadda, D. Giuricin, G., Mardirossian, F., & Mezzetti, M., 1997a, *ApJ*, 482, 41
- Girardi, M., Fadda, D., Escalera, E., Giuricin, G., Mardirossian, F., & Mezzetti, M. 1997b, *ApJ*, 490, 56
- Girardi, M., Fadda, D., Giuricin, G., Mardirossian, F., Mezzetti, M., & Biviano, A. 1996, *ApJ*, 457, 61
- Girardi, M., Giuricin, G., Mardirossian, F., Mezzetti, M., & Boschin, W. 1998b, *ApJ*, 505, 74 (G98)
- Gunn, J. E., Hoessel, J. G., & Oke, J. B. 1986, *ApJ*, 306, 30
- Henry, J. P. 1997, *ApJ*, 489, L1
- Henry, J. P., Gioia, I. M., Maccacaro, T., Morris, S. L., Stocke, J. T., & Wolter, A. 1992, *ApJ*, 386, 408
- Hoekstra, H., Franx, M., Kuijken, K., & Squires, G. 1998, *ApJ*, 504, 636

- Infante, L., Fouqué, P., Hertling, G., Way, M. J., Giraud, E., & Quintana, H. 1994, *A&A*, 289, 381
- Isobe, T., Feigelson, E. D., Akritas, M. G., & Babu, G. J. 1990, *ApJ*, 364, 104
- Jones, Ebeling, H., Scharf, C., Perlman, E., Horner, D., Fairley, G., Wegner, G., & Malkan, M. 2000, astro-ph/0001376
- Jones, C., & Forman, W. 1992, in *Clusters and Superclusters of Galaxies*, ed. A. C. Fabian (Dordrecht: Kluwer), 49
- Jones, C., & Forman, W. 1999, *ApJ*, 511, 65
- Jones, L. R., Schraf, C., Ebeling, H., Perlman, E., Wegner, G., Malkan, M., & Horner, D. 1998, *ApJ*, 495, 100
- Kaiser, N., Wilson, G., Luppino, G., Kofman, L., Gioia, I. M., Metzger, M., & Dahle, H. 1998, preprint astro-ph/9809268
- Katgert, P., Mazure, A., den Hartog, R., Adami, C., Biviano, A., & Perea, J. 1998, *A&AS*, 129, 399
- Kolokotronis, V., Basilakos, S., Plionis, M., & Georgantopoulos, I. 2000, submitted to *MNRAS*, preprint astro-ph/0002432
- Koranyi, D. M., & Geller, M. J. 2000, *AJ*, 119, 44
- Lea, S. M., & Henry, J. P. 1988, *ApJ*, 332, L81
- Le Borgne, J.-F., Pelló, R., & Sanahuja, B. 1992, *A&AS* 95, 87
- Lemonon, L., Pierre, M., Hunstead, R., Reid, A., Mellier, Y., & Böhringer, H. 1997, *A&A*, 326, 34
- Lewis, A. D., Ellingson, E., Morris, S. L., & Carlberg, R. G. 1999, *ApJ*, 517, 587
- Limber, D. N., & Mathews, W. G. 1960, *ApJ*, 132, 286
- Lombardi, M. et al. 2000, in prep.
- Lubin, L. M., Postman, M., & Oke, J. B. 1998a, *AJ*, 116, 643
- Lubin, L. M., Postman, M., Oke, J. B., Ratnatunga, K. U., Gunn, J. E., Hoessel, J. G., Schneider, D. P. 1998b, *AJ*, 116, 584
- Lumsden, S. L., Nichol, R. C., Collins, C. A., & Guzzo, L. 1992, *MNRAS*, 258, 1
- Luppino, G. A., & Kaiser, N. 1997, *ApJ*, 475, L20
- Maurogordato, S., Proust, D., Beers, T. C., Arnaud, M., Pelló, R., Cappi, A., Slezak, E., & Kriessler, J. R. 1999, preprint astro-ph/9903476
- Merritt, D. 1988, in *The Minnesota Lectures on Clusters of Galaxies and Large-Scale Structures*, ed. J. M. Dickey (ASP Conf. Ser., 5), p. 175
- Miralda-Escudé, J., & Babul, A. 1995, *ApJ*, 449, 18
- Mohr, J. J., Geller, M. J., Fabricant, D. G., Wegner, G., Thorstensen, J., & Richstone, D. O. 1996, *ApJ*, 470, 724
- Moss, C., & Dickens, R. J. 1977, *MNRAS*, 178, 701
- Mushotzky, R. F. 2000, *Astr. Soc. of the Pacific Conf. Ser.*, 193, 323
- Mushotzky, R. F., & Scharf, C. A. 1997, *ApJ*, 482, L13
- Mushotzky, R. F., & Loewenstein, M. 1997, *ApJ*, 481, L63
- Natarajan, P., Kneib, J.-P., Smail, I., & Ellis, R. S. 1998, *ApJ*, 499, 600
- Oegerle, W., Fitchett, M. J., Hill, J. M., Hintzen, P. 1991, *ApJ*, 376, 460
- Ostrander, E. J., Nichol, R. C., Ratnatunga, K. U., & Griffiths, R. E. 1998, *AJ*, 116, 2644
- Oukbir, J., & Blanchard, A. 1992, *A&A*, 252, L21
- Pierre, M., Matsumoto, H., Tsuru, T., Ebeling, H., & Hunstead, R. 1999, *A&AS*, 136, 173
- Pisani, A. 1993, *MNRAS*, 265, 706
- Pisani, A. 1996, *MNRAS*, 278, 697
- Postman, M., Lubin, L., Gunn, J. E., Oke, J. B., Hoessel, J. G., Schneider, D. P., & Christensen, J. A. 1996, *AJ*, 111, 615
- Postman, M., Lubin, L. M., & Oke, J. B. 1998, *AJ*, 116, 560
- Press, W. H., Teukolsky, S. A., Vetterling, W. T., & Flannery, B. P. 1992, *Numerical Recipes* (2d ed.; Cambridge: Cambridge Univ. Press)
- Proust, D., Cuevas, H., Capelato, H. V., Sodr , L. Jr., Tom  Lehodey, B., Le F vre, O., & Mazure, A. 2000; *A&A*, 355, 443
- Rosati, P., Borgani, S., Della Ceca, R., Stanford, S. A., isenhardt, P. R., & Lidman, C. 2000, astro-ph/0001119
- Rosati, P., Stanford, S. A., Eisenhardt, P. R., Elston, R., Spinrad, H., Stern, D., & Dey, A. 1999, *AJ*, 118, 76
- Rosati, P., S., Della Ceca, R., Norman, C., & Giacconi, R. 1998, *ApJ*, 492, L21
- Schindler, S. 1999, *A&A*, 349, 435
- Seitz, C., Kneib, J.-P., Schneider, P., & Seitz, S. 1996, *A&A*, 314, 707
- Smail, I., Ellis, R. S., dressler, A., Couch, W. J., Oemler, A. Jr., Sharples, R. M., & Butcher, H. 1997, *ApJ*, 479, 70
- Solanes, J. M., Salvador-Sol , E., & Gonz lez-Casado, G. 1999, *A&A*, 343, 733
- Soucail, G., Ota, N., B hringer, H., Czoske, O., Hattori, M., & Mellier, Y. 2000, *A&A*, 355, 433
- Squires, G., Kaiser, N., Babul, A., Fahlman, G., Woods, D., Neumann, D. M., & B hringer 1996a, *ApJ*, 461, 572
- Squires, G., Kaiser, N., Fahlman, G., Babul, A., & Woods, D. 1996b, *ApJ*, 469, 73
- Taylor, A. N., & Dye, S., Broadhurst, T. J., Benitez, N., & van Kampen, E. 1998, *ApJ*, 501, 539
- Teague, P. F., Carter, D., & Gray, P. M. 1990, *ApJS*, 72, 715
- The, L. S., & White, S. D. M. 1986, *AJ*, 92, 1248
- Tran, K.-V. H., Kelson, D. D., van Dokkum, P., Franx, M., Illinworth, G. D., & Magee, D. 1999, *ApJ*, 522, 39
- Tucker, W., et al. 1998, *ApJ*, 496, L5
- Ulmer, M. P., Cruddace, R. G., & Kowalski, M. P. 1985, *ApJ*, 290, 551
- Vikhlinin, A., McNamara, B. R., Forman, W., Jones, C., Quintana, H., & Hornstrup, A. 1998, *ApJ*, 498, L21
- White, R. E. III 1991, *ApJ*, 367, 69
- White, D. A., Jones, C., & Forman, W. 1997, *MNRAS*, 292, 419
- Wu, X. P., & Fang, L. Z., 1996, *ApJ*, 467, 45
- Wu, X. P., & Fang, L. Z., 1997, *ApJ*, 483, 62
- Wu, X. P., Fang, L. Z., & Xue, Y. 1998, *MNRAS*, 301, 861
- Wu, X. P., Xue, Y., & Fang, L. Z. 1999, *ApJ*, 524, 22
- Yaqoob, T. 1999, *ApJS*, 120, 179
- Yee, H. K. C., Ellingson, E., Abraham, R., Gravel, P., Carlberg, R. G., Smecker-Hane, T. A., Schade, D., & Rigler, M. 1996a, *ApJS*, 102, 289
- Yee, H. K. C., Ellingson, E., & Carlberg, R. G. 1996b, *ApJS*, 102, 269
- Yee, H. K. C., Ellingson, E., Morris, S. L., Abraham, R., & Carlberg, R. G. 1998, *ApJS*, 116, 211
- Zabludoff, A. I., Huchra, J. P., & Geller, M. J. 1990, *ApJS*, 74, 1
- Zwicky, F., Herzog, E., Wild, P., Karpowicz, M., & Kowal, C. 1961 - 1968, *Catalog of Galaxies and of Clusters of Galaxies*, vol.s 1-6 (Pasadena: California Institute of Technology)